

# Current advances in ligand design for inorganic positron emission tomography tracers $^{68}\text{Ga}$ , $^{64}\text{Cu}$ , $^{89}\text{Zr}$ and $^{44}\text{Sc}$

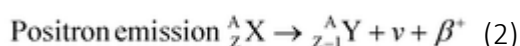
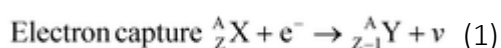
Thomas W. Price John Greenman and Graeme J. Stasiuk

## Abstract

A key part of the development of metal based Positron Emission Tomography probes is the chelation of the radiometal. In this review the recent developments in the chelation of four positron emitting radiometals,  $^{68}\text{Ga}$ ,  $^{64}\text{Cu}$ ,  $^{89}\text{Zr}$  and  $^{44}\text{Sc}$ , are explored. The factors that effect the chelation of each radio metal and the ideal ligand system will be discussed with regards to high in vivo stability, complexation conditions, conjugation to targeting motifs and complexation kinetics. A series of cyclic, cross-bridged and acyclic ligands will be discussed, such as CP256 which forms stable complexes with  $^{68}\text{Ga}$  under mild conditions and PCB-TE2A which has been shown to form a highly stable complex with  $^{64}\text{Cu}$ .  $^{89}\text{Zr}$  and  $^{44}\text{Sc}$  have seen significant development in recent years with a number of chelates being applied to each metal – eight coordinate di-macrocyclic terephthalamide ligands were found to rapidly produce more stable complexes with  $^{89}\text{Zr}$  than the widely used DFO.

## 1. Introduction

Positron Emission Tomography (PET) is a medical diagnostic technique that is dependent on the decay of neutron deficient nuclei that are introduced into the body as a radiotracer. Neutron deficient nuclei can undergo two different decay processes – electron capture (eqn (1)) and positron emission (eqn (2)).



PET exploits the second of these – the emitted positron travels a short distance (the average positron emitted by  $^{18}\text{F}$  travels 0.6 mm whereas one emitted by  $^{68}\text{Ga}$  travels 2.9 mm)<sup>1</sup> and then undergoes an annihilation interaction with an electron nearby.<sup>2</sup> The annihilation interaction results in two  $\gamma$  photons, each with an energy of 511 keV,<sup>2</sup> being emitted simultaneously at 180° to each other.<sup>2</sup> These two photons can be detected and a “line of coincidence” constructed to localise their source. The collection of millions of such events allows for the construction of a PET image (Fig. 1).<sup>3</sup>

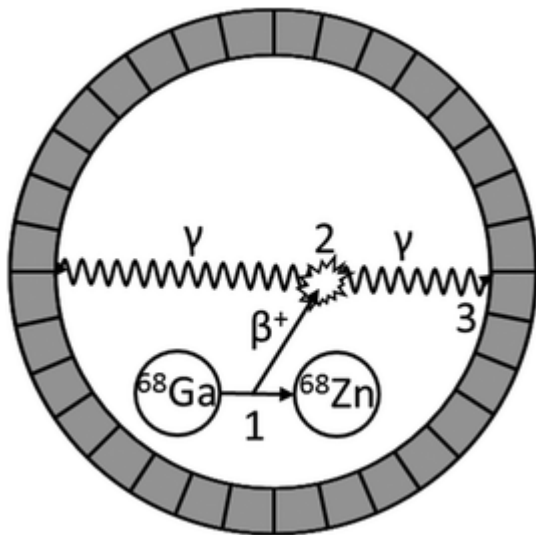


**Fig. 1** Schematic of a PET imaging process. 1. Positron emitted from radionuclide. 2. Positron and electron undergo annihilation interaction and emit two photons. 3. Emitted photons detected.<sup>8</sup>

As an imaging technique PET has a number of advantages – chief amongst these is its high sensitivity.<sup>4,5</sup> A key advantage of the high sensitivity of PET is that this leads to a very small dose of the tracer being required – for the imaging of adults, a dosage of 370–740 MBq of <sup>18</sup>F-FDG is typical,<sup>6</sup> this corresponds to approximately 6 pmol of the radiotracer. This is beneficial as it reduces any toxicity concerns and ensures that PET tracers do not saturate biological receptors. PET can also be used as a quantitative technique allowing for in depth study of physiological processes.<sup>7</sup>

Recently, a number of positron emitting metal isotopes (Table 1) have begun to find widespread use in research<sup>8</sup> and are moving towards medical applications. These PET isotopes have found favour due to their longer half-lives in comparison to the common organic PET isotopes <sup>11</sup>C and <sup>18</sup>F (Table 1) – this allows them to be produced off-site and transported to the imaging location, potentially allowing for a single production facility supplying a number of medical facilities.

**Table 1** Properties of a selection of positron emitting isotopes

Nucleus	Half-life/minutes <sup>9</sup>	Production	Decay modes /keV	$E_{\beta^+}^{\text{Mean}}$
<sup>11</sup> C	20	<sup>14</sup> N(p, α) <sup>11</sup> C cyclotron <sup>3</sup>	β <sup>+</sup> 100% <sup>9</sup>	390 <sup>10,11</sup>
<sup>18</sup> F	110	<sup>18</sup> O(p, n) <sup>18</sup> F cyclotron <sup>3</sup>	β <sup>+</sup> 100% <sup>9</sup>	252, <sup>10</sup> 250 <sup>11</sup>
<sup>44</sup> Sc	238	<sup>44</sup> Ti/ <sup>44</sup> Sc generator	β <sup>+</sup> 100%	632 <sup>12,13</sup>
		<sup>44</sup> Ca(p, n) <sup>44</sup> Sc cyclotron		

Nucleus	Half-life/minutes <sup>9</sup>	Production	Decay modes	/keV
<sup>64</sup> Cu	762	<sup>64</sup> Ni(p, n) <sup>64</sup> Cu cyclotron <sup>8</sup>	$\beta^+$ 19% EC 41% $\beta^-$ 40% <sup>8</sup>	278 <sup>12</sup>
<sup>68</sup> Ga	68	<sup>68</sup> Ge/ <sup>68</sup> Ga generator <sup>8</sup>	$\beta^+$ 90% EC 10% <sup>8</sup>	830 <sup>11,12</sup> , 844 <sup>10</sup>
<sup>89</sup> Zr	4710	<sup>89</sup> Y(p, n) <sup>89</sup> Zr <sup>8</sup>	$\beta^+$ 23% EC 77% <sup>8</sup>	397 <sup>14</sup>

The longer half-life of these isotopes also allows for the study of slower biological processes, but will prevent repeated imaging in a short space of time. The incorporation of ionic metal isotopes into a PET tracer is through a complexation mechanism, with the synthesis of the rest of the tracer being undertaken on a larger scale using cold chemistry.

In order to successfully apply these metal nuclei to imaging of biological processes they must be chelated in an organic framework and bound to a targeting motif. This chelation is important for a number of reasons – the targeting of specific biomarkers depends on the pairing of the PET isotope with the relevant targeting species. If the PET tracer is not bound it will result in the signal being linked to blood flow and where the metal naturally accumulates (e.g. copper accumulates in the liver).<sup>15</sup> Alternatively, if the metal is picked up by another biological molecule (e.g. gallium by transferrin)<sup>16</sup> it may result in imaging an entirely different biological process. As a result, the careful selection of both chelate and targeting motif is important when developing an imaging agent. The selection of chelate will depend upon the metal used, which in turn will often be decided by the half-life required for the study in question. The targeting motif will depend on the receptor being studied and this may influence the selection of the other components of the tracer.

The complexation of radiometals, such as <sup>64</sup>Cu and <sup>68</sup>Ga, is a key requirement for the development of targeted radiotracers that can be used in vivo. The chelate-metal complex must fulfil several key requirements:

## 1.1 Rapid complexation

$^{68}\text{Ga}$  has a half-life of just 68 minutes – an effective tracer that uses this radio nuclei needs to be ready soon after it is produced. Rapid formation and purification of the chelate-metal complex is one of the key areas being developed in this field.<sup>17</sup>

## 1.2 Mild complexation conditions

Many of the targeting vectors used are susceptible to decomposition under the harsh conditions often required for rapid chelation. As such, high temperatures and extreme pH values are to be avoided. While it is possible to conjugate the complex to the probe after radiolabelling,<sup>18</sup> this is typically not favoured as it results in a longer synthetic period overall.

## 1.3 High in vivo stability

This is essential if the radiometal is to have any specific targeting ability. The metal-chelate complex must be stable to transmetallation by biochelators (e.g. metalloproteins).<sup>16</sup> If the radiometal is displaced from the chelate complex it will no longer be specifically targeted. Weakly coordinated gallium is seen to accumulate in the skeleton,<sup>19,20</sup> whereas copper accumulates in the liver.<sup>15,21</sup>

## 1.4 Readily conjugated to targeting motifs

In order to be used efficiently as imaging agents the radiotracers will need to specifically target biomarkers that indicate the disease state that is being studied. Whilst there are examples of chelates that will target disease states automatically,<sup>22,23</sup> it is more common to use a bifunctional chelator (BFC) that can be conjugated to a targeting vector. Care must be taken during this step to avoid disrupting the chelation properties of the BFC. In some extreme cases, the conjugation can take place in the body.<sup>24</sup> This review will not explore the various bioconjugation techniques that are used in the field of molecular imaging,<sup>25</sup> but where possible will highlight successful incorporation of a site for conjugation into a chelate.

Each radiometal used has its own specific requirements for optimal chelation – and each also has its own challenges. This review will discuss the chelation of  $^{68}\text{Ga}$ ,  $^{64}\text{Cu}$ ,  $^{89}\text{Zr}$  and  $^{44}\text{Sc}$ . The coordination of radiometals, including  $^{68}\text{Ga}$ ,  $^{64}\text{Cu}$  and  $^{89}\text{Zr}$ , was extensively reviewed in 2010 by Anderson and coworkers<sup>8</sup> and more recently Price and Orvig covered the coordination of a range of radiometals.<sup>17</sup>

## 2. Gallium-68

The popularity of  $^{68}\text{Ga}$  as a radiotracer for PET can be attributed to the development of the  $^{68}\text{Ge}/^{68}\text{Ga}$  generator which produces  $^{68}\text{Ga}$  through the decay of  $^{68}\text{Ge}$ .<sup>20</sup> This generator combines a long lived “parent” radioisotope ( $^{68}\text{Ge}(\text{IV}) - t_{1/2} = 271$  days) with a “daughter isotope” which has very different chemical properties and a half-life suitable for medical imaging ( $^{68}\text{Ga}(\text{III}) - t_{1/2} = 68$  minutes).<sup>20</sup> These two metals can be readily separated with the parent remaining on the generator column and the daughter being eluted with concentrated hydrochloric acid.<sup>20</sup> This provides a non-cyclotron based route to a positron emitter, allowing for research and diagnosis to be undertaken at sites lacking the specialist cyclotron-based equipment normally required for PET. This development of  $^{68}\text{Ga}$  based PET imaging has the potential to be extremely beneficial to the field of medical imaging as the generator based production of  $^{68}\text{Ga}$  would be suitable for implementation in hospitals.<sup>26</sup> Successful application of a generator produced radioisotope to diagnostic imaging has already been seen with the highly popular  $^{99\text{m}}\text{Tc}$  isotope;<sup>27</sup> repeating this success with  $^{68}\text{Ga}$  would lead to a readily available PET imaging.

In aqueous solutions the only stable oxidation state of gallium is  $\text{Ga}(\text{III})$  which is present as the hydrate complex under acidic conditions.<sup>20</sup> In the pH range 3–7, this readily forms the complex  $\text{Ga}(\text{OH})_3$  which is highly insoluble<sup>20</sup> – this is a concern during the chelation step, which must be rapid due to the short half-life of  $^{68}\text{Ga}$ , as the transchelation of  $\text{Ga}(\text{III})$  from  $\text{Ga}(\text{OH})_3$  is slow.<sup>19</sup> At physiological pH  $[\text{Ga}(\text{OH})_4]^-$  is formed instead, which is soluble in water<sup>20</sup> but still displays slow chelation kinetics due to the strong coordination of hydroxyl ligands to gallium.<sup>19</sup> As such, chelation studies are usually undertaken under conditions that prevent the formation of  $\text{Ga}(\text{OH})_3$ <sup>20</sup> or in the presence of a “trapping” ligand such as citrate or acetate.<sup>19,20</sup>

Many of the properties of six coordinate  $\text{Ga}(\text{III})$  are very similar to high spin  $\text{Fe}(\text{III})$  (Table 2) – this is the source of a number of issues in vivo as metalloproteins that typically chelate iron will also chelate  $\text{Ga}(\text{III})$  strongly.  $\text{Ga}(\text{III})$  shows a strong affinity for transferrin,<sup>16</sup> an important iron transporter in humans. This affinity defines much of the work that has been undertaken in the field of gallium chelation as it provides a standard against which a successful chelate must positively compare. Transchelation of  $^{68}\text{Ga}$  by transferrin would result in a loss of specificity and an accumulation of  $^{68}\text{Ga}$  in the liver, lungs and bone.<sup>19,20</sup>

**Table 2** Comparison of properties of  $\text{Ga}(\text{III})$  and  $\text{Fe}(\text{III})$

Property	$\text{Ga}(\text{III})$	$\text{Fe}(\text{III})$
Ionic configuration	$[\text{Ar}] 3d^{10}$ (ref. 8)	$[\text{Ar}] 3d^5$
Ionic radius (6 coordinate)	$62^{19}$	$65^{19}$
Log $K_{\text{Transferrin-M-1}}$	$20.3^{16,19}$	$22.8^{19}$

Property	Ga(III)	Fe(III)
Log $K_{\text{Transferrin-M-2}}$	19.3 <sup>16,19</sup>	21.5 <sup>19</sup>

Ga(III) typically has a coordination number of 6 and complexes that fulfil this will have an octahedral coordination geometry.<sup>28</sup> Due to its high charge and small ionic radius, the Ga(III) ion is classified as a hard Lewis acid.<sup>19</sup> Therefore, it is expected that Ga(III) will display a high thermodynamic stability in complexes with hard Lewis basic sites containing atoms such as oxygen and nitrogen which can donate a lone pair of electrons to the Ga(III) ion. Carboxylate,<sup>29</sup> phosphonate,<sup>30</sup> and amine<sup>31,32</sup> groups are ideal, and phenolate<sup>32</sup> and thiol<sup>29,33,34</sup> groups have shown some success at chelating Ga(III) as well (Table 3).

**Table 3** Stability of gallium-chelator complexes

Chelator	Coordinating atoms	Log $K_{\text{Ga-L}}$
Transferrin	NO <sub>5</sub>	20.3 <sup>16</sup>
NOTA	N <sub>3</sub> O <sub>3</sub>	31.0 <sup>8,37</sup>
TACN-TM	N <sub>3</sub> S <sub>3</sub>	34.2 <sup>8,38</sup>
DOTA	N <sub>4</sub> O <sub>2</sub>	26.1 <sup>39</sup>
TETA	N <sub>4</sub> O <sub>2</sub>	19.7 <sup>8,40</sup>
EDTA	N <sub>2</sub> O <sub>4</sub>	22.0 <sup>41</sup>
ED2A2M	N <sub>2</sub> O <sub>2</sub> S <sub>2</sub>	31.6 <sup>33</sup>
HBED	N <sub>2</sub> O <sub>4</sub>	37.7 <sup>8,42</sup>
EC	N <sub>2</sub> O <sub>2</sub> S <sub>2</sub>	31.5 <sup>29</sup>
DTPA	N <sub>3</sub> O <sub>3</sub>	25.1 <sup>41</sup>
SBAD	N <sub>4</sub> O <sub>2</sub>	28.3 <sup>32</sup>

## 2.1. First generation chelates for <sup>68</sup>Ga

A number of cyclic chelates (Fig. 2) have been studied with <sup>68</sup>Ga – particularly those based on the 14710-tetraazacyclododecane-N,N',N'',N'''-tetraacetic acid (DOTA – Fig. 2)<sup>35</sup> and 1,4,7-triazacyclononane-N,N',N''-triacetic acid (NOTA – Fig. 2)<sup>36</sup> frameworks. These systems have shown a high kinetic inertness, but exhibit poor chelation kinetics – requiring either a long complexation time or harsh conditions, neither of these are ideal for the development of radiotracers

containing biomolecules. Development of these cyclic systems has aimed to improve the chelation kinetics without squandering the kinetic inertness of the resulting complex.<sup>43,44</sup>

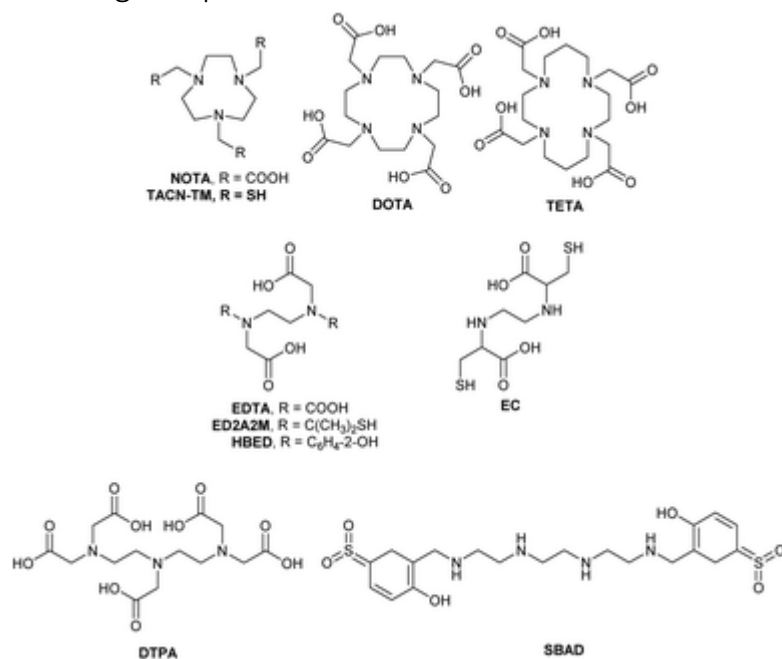


**Fig. 2** Structures of gallium chelators.

In contrast, acyclic chelates show more favourable complex formation kinetics under mild conditions, but weaker complex stability under biological conditions. Development of acyclic chelates for <sup>68</sup>Ga has thus had the opposite problem – development in this area has focused on improving complex stability whilst maintaining the rapid complex formation that is associated with these acyclic chelates.<sup>4,45</sup>

Some conclusions can be drawn from the early work in this field (Table 3) that may be of benefit when considering future chelate design. The expansion of the azamacrocyclic ring from NOTA to DOTA and 1,4,8,11-tetraazacyclotetradecane-N,N',N'',N'''-tetraacetic acid (TETA – Fig. 2) results in a drastic drop in the stability of the complex formed of log 10 units from log  $K_{\text{Ga-NOTA}} = 31.0$ <sup>37</sup> to log  $K_{\text{Ga-DOTA}} = 26.1$ <sup>39</sup> and log  $K_{\text{Ga-TETA}} = 19.7$ .<sup>58</sup> This demonstrates the importance of a cavity size – ionic radius match in the thermodynamic stability of the complex formed.

Comparing NOTA to the trismercaptoptriazacyclononane chelate (TACN-TM – Fig. 2) shows the viability of thiol groups as chelating ligands for Ga(III) as the thiol containing chelate shows a higher stability (log  $K_{\text{Ga-TACN-TM}} = 34.2$ )<sup>38</sup> than the carboxylic acid derivative NOTA. A comparison of two acyclic chelates, ethane-1,2-diamine-N,N',N'-tetraacetic acid (EDTA – Fig. 2)<sup>41</sup> and N,N'-bis(2,2'-dimethyl-2-mercaptoethyl)ethylenediamine-N,N'-diacetic acid (ED2A2M – Fig. 2),<sup>33</sup> reveals the same trend with the thiol containing chelate being much more stable (log  $K_{\text{Ga-}}$

$\text{ED2A2M} = 31.6)^{33}$  than the carboxylate containing chelate ( $\log K_{\text{Ga-EDTA}} = 22.0$ ).<sup>41</sup> However the phenol containing system HBED (Fig. 2) shows even greater stability with  $\log K_{\text{Ga-HBED}} = 37.7$ .<sup>42</sup> Despite this greater stability, few systems using phenols and thiols as coordinating ligands have been used to chelate gallium. This may be due to their low acidity in comparison to carboxylic acids ( $\text{pK}_a$  ethanethiol = 10.5,  $\text{pK}_a$  phenol = 9.95,  $\text{pK}_a$  Acetic Acid = 4.76)<sup>46</sup> resulting in poor coordination kinetics under the acidic labelling conditions required to prevent the formation of  $\text{Ga}(\text{OH})_3$ .

A comparison of N,N'-ethylene-di-L-cysteine (EC – Fig. 2,  $\log K_{\text{Ga-EC}} = 31.5$ ),<sup>29</sup> in which the thiol containing arms are connected to the carbon back bone, and ED2A2M,<sup>33</sup> in which they are connected to the amine groups, reveals little difference in stability – overall the same groups are donating electron density to the Ga(III) ion and the cavity size should be similar so this is not entirely surprising.

## 2.2. Developments in $^{68}\text{Ga}$ chelator design

2.2.1. Macrocyclic chelators. Much of the work involving cyclic chelates has been aimed towards medical applications. The DO3Am core (Fig. 3), in which one of the pendant acidic groups of DOTA has been conjugated through a peptide bond, shows significantly lower chemical stability than the original chelate ( $\log K_{\text{Ga-DOTA}} = 26.1$ ,  $\log K_{\text{Ga-DO3AmBu}} = 24.6$ ).<sup>39,47</sup> This is surprising as the model for Ga-DOTA binding has two of the pendant arms not being directly involved in the chelation. Nonetheless, this system has been applied to targeted imaging,<sup>47-50</sup> including applications in diagnosis of human patients. A bicyclic somatostatin agonist was conjugated to  $^{68}\text{Ga-DO3Am}$  and showed high tumour and kidney uptake. The tumour uptake could be blocked by injection with DOTANOC (vide infra) and the kidney uptake by injection with lysine to reduce background signal.<sup>48</sup> DO3Am functionalised with bisphosphonate was used in an in-man study to highlight osteoblastic lesions caused by prostate cancer metastases.<sup>47</sup> DOTATOC, DOTANOC and DOTATATE are all derivatives of DO3AM with specific peptide sequences for the targeting of somatostatin receptors. DOTATOC has the sequence D-Phe-Cys-Tyr-D-Trp-Lys-Thr-Cys-Thr(OH), DOTANOC has the sequence D-Phe-Cys-Nal-D-Trp-Lys-Thr-Cys-Thr(OH) and DOTATATE has the sequence D-Phe-Cys-Tyr-D-Trp-Lys-Thr-Cys-Thr.  $^{68}\text{Ga}$  complexes of all three have been applied in a number of medical studies.<sup>51-55</sup>

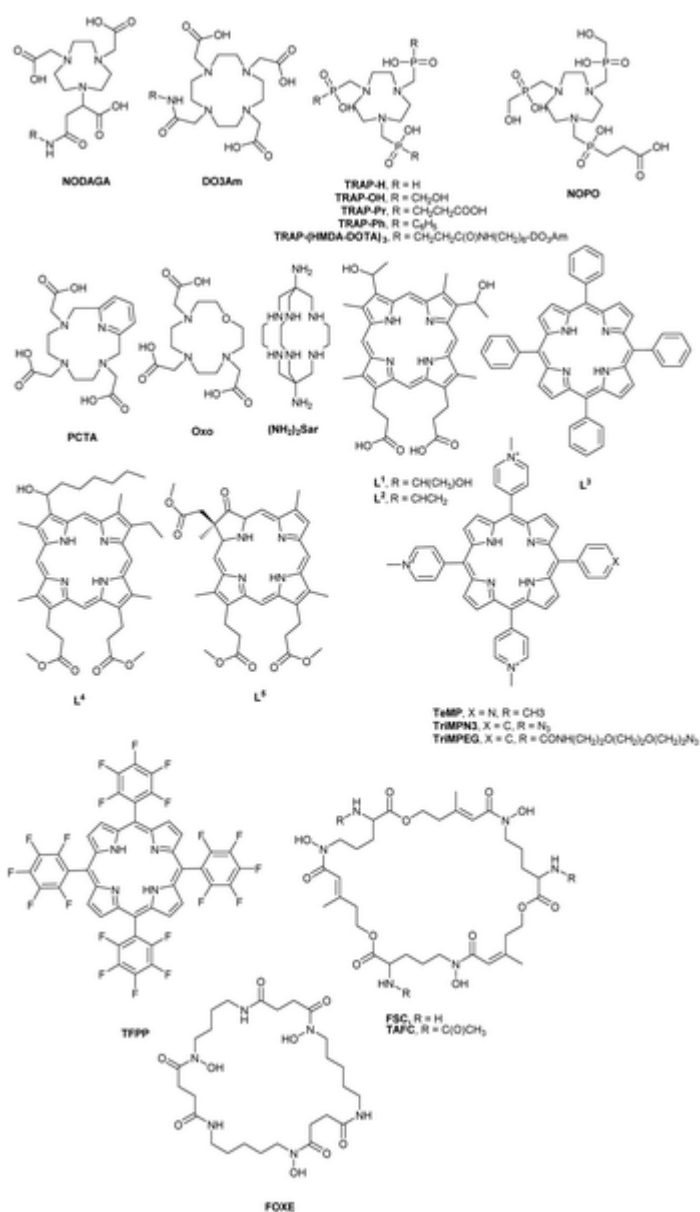


**Fig. 3** Structures of novel cyclic gallium chelators.

NOTA was conjugated from the macrocyclic carbon backbone in multiple studies – the labelling properties and stability of these complexes were found to be good, with labelling proceeding at room temperature in 10 minutes.<sup>56</sup> Minimal transfer to transferrin was seen in *in vitro* tests with these chelates.<sup>56</sup> When functionalised with nitrobenzene the complex showed high retention in the kidneys and the bladder, but also showed rapid clearance from blood, heart and muscle.<sup>57</sup> When conjugated to c(RGDyK) this system showed no degradation over 2 hours, and only 2% over 3 hours, in the presence of transferrin at 37 °C and pH 6.9.<sup>58</sup> When a bisphosphonate functionality was applied to NOTA through C-functionalisation of a pendant arm, the resulting complex showed good blood clearance and some uptake in the skeleton 2 hours after injection.<sup>59</sup> The stability of this system was very high, 95% of the original complex remained after 3 hours in rat plasma. This

was applied to the imaging of osteolytic lesions in mice<sup>59</sup> as well as being applied to an in man study<sup>47</sup> showing high target uptake and low soft tissue uptake.

A commonly used NOTA derivative is NODAGA (Fig. 3)<sup>60</sup> showing similar complexation kinetics to NOTA,<sup>49,50,61,62</sup> NODAGA has been chelated to a number of different peptides including c(RGDyK), c(RGDfK) and Nal3-octretide (NOC) and also to bisphosphonate.<sup>49,50,59,61,62</sup> These derivatives showed good stability, due to their NOTA core, and high target uptake in small mammal models, with <sup>68</sup>Ga-NOTA-LM3 showing a 10 fold greater somatostatin receptor uptake than the equivalent <sup>68</sup>Ga-DOTA-LM3 system.<sup>50</sup>

The adaptation of NOTA to include phosphonic acids and phosphinates to form the TRAP system (Fig. 3) by Notni and coworkers<sup>30,63</sup> led to a chelate that could be labelled with <sup>68</sup>Ga across a range of conditions. Of particular interest is the potential to label under extremely acidic conditions, such as those of the eluent from the <sup>68</sup>Ge/<sup>68</sup>Ga generator. This is possible due to the low pK<sub>a</sub> of the phosphinic acids (pK<sub>a</sub> < 1) used in the TRAP chelates.<sup>63</sup> TRAP-Pr, in which the phosphinate is capped with butanoic acid, equilibrated very slowly. After weeks of equilibration this gave a stability constant, log K<sub>Ga-TRAP-Pr</sub> = 26.2, however on the time scale of <sup>68</sup>Ga imaging the value was approximated to be log K<sub>Ga-TRAP-Pr</sub> = 35, which is higher than the reported value for Ga(III)-NOTA (log K<sub>Ga-NOTA</sub> = 31.0).<sup>37</sup> The proposed reason for this high stability is the increased negative charge of the [Ga(III)-TRAP]<sup>3-</sup> species relative to Ga(III)-NOTA – this would hinder the approach of hydroxide anions and therefore decomplexation of the Ga(III) ions.

Amide coupling performed on the pendant carboxylate groups of TRAP-Pr allowed the conjugation of c(RGDyK) to this chelate without affecting the binding site.<sup>62,64</sup> Notni and coworkers demonstrated that conjugation using a copper catalysed “click” mechanism was a feasible means of conjugating the TRAP chelate to peptides.<sup>65</sup> While the copper catalyst used was bound by the TRAP chelate, this could be removed using a more thermodynamically stable chelator prior to radiolabelling.<sup>65</sup> A compound with both rhodamine and c(RGDyK) conjugated and a third with biotin chelated were also formed.<sup>30</sup> The tris-RGD compound showed a much higher affinity for α<sub>v</sub>β<sub>3</sub> receptors than <sup>68</sup>Ga-NODAGA-RGD or <sup>18</sup>F-galacto-RGD with the inhibition concentration of TRAP-(RGD)<sub>3</sub> being an order of magnitude lower.<sup>64</sup> A multimodal PET-MRI agent based on the TRAP chelate has been developed in which DOTA was attached to the end of the pendant arms. Complexation with gadolinium resulted in both the TRAP and DOTA sites being occupied by Gd(III). Ga(III) could displace the Gd(III) in the central TRAP site relatively easily, forming the [Ga][Gd]<sub>3</sub>[TRAP-(HMDA-DOTA)<sub>3</sub>] complex. For the purposes of radiolabelling, the central Gd(III) ion was removed by addition of DTPA before addition of <sup>68</sup>Ga to form [<sup>68</sup>Ga][Gd]<sub>3</sub>[TRAP-(HMDA-DOTA)<sub>3</sub>].<sup>66</sup> Due to the

significant difference in sensitivity of MRI and PET, 20  $\mu\text{mol}$  of  $[\text{Gd}]_4[\text{TRAP}-(\text{HMDA-}\text{DOTA})_3]$  was injected along with 0.8 nmol of the  $^{68}\text{Ga}[\text{Gd}]$  complex during rat studies in which both PET and MRI images could be collected with colocalised regions of contrast.<sup>66</sup>

A derivative of the TRAP chelate in which the pendant arms are different is NOPO (Fig. 3). In this asymmetric chelate two of the arms are methyl alcohol groups whereas the third is a butanoic acid species<sup>67</sup> This had little effect on the stability and coordination properties of this species compared to TRAP – perhaps not surprising as both TRAP-OH and TRAP-Pr showed good properties in both of these areas – however this asymmetric functionalization allows for the selective conjugation of the carboxylic acid arm to give a mono-peptide chelate.<sup>44,68</sup> This allows for the direct comparison of this chelate to other mono-peptides, such as DOTATOC, and also has the potential to allow a multimodal imaging agent to be made through selective functionalization of the carboxylic and alcohol arms. RGD-chelated<sup>68</sup>Ga-NOPO was shown to have high hydrophilicity and cleared rapidly from the blood and organs of mice.<sup>44</sup> Chelation to NaI3-octretide to create NOPO-NOC yielded a gallium complex that showed high tumour uptake and low organ uptake in rats.<sup>68</sup>

PCTA (Fig. 3) incorporates pyridine into the macrocycle of DOTA in place of a secondary amine.<sup>58</sup> PCTA-RGD was labelled with <sup>68</sup>Ga in under 30 minutes at room temperature and is reasonably stable to transferrin, with 10% of <sup>68</sup>Ga being lost in 4 hours.<sup>57</sup> <sup>57</sup>Ga-PCTA-RGD displayed a similar biodistribution to Ga-NOTA-RGD, but exhibited lower kidney uptake and a higher tumour-to-kidney ratio – this is encouraging for future work as this will improve the contrast of any collected images.

2,2',2''-(1-Oxa-4,7,10-triazacyclododecane-4,7,10-triyl)triacetic acid (oxo – Fig. 3), in which one of the aza nitrogens of DOTA is replaced with an oxygen atom, was far less stable and showed significant degradation in the presence of transferrin.<sup>57</sup>

Typically used with copper and other metals, Ma and coworkers used (c(RGDyK)NH)<sub>2</sub>Sar with <sup>68</sup>Ga to some success.<sup>69</sup> Radiolabelling required 30 minutes incubation at 80 °C, but the resultant complex was relatively stable to transferrin after incubation for 2 hours, with only 11% of the complex degrading (Table 4).

**Table 4** Stability and radiochemical yield (RCY) of macrocyclic chelates for <sup>68</sup>Ga chelation

Chelator	Log K <sub>ML</sub>	Labelling conditions	RCY/%
DOTA	26.1 <sup>39</sup>	85 °C, pH 4.0, 30 minutes, 100 $\mu\text{M}$	95 <sup>70</sup>
DO3Am	24.6 <sup>39</sup>	80 °C, pH 4, 5 minutes, 1 mM	100 <sup>71</sup>

Chelator	Log K <sub>ML</sub>	Labelling conditions	RCY/%
NOTA	31.0 <sup>8,37</sup>	RT, pH 3.5, 10 minutes, 10 μM	95 <sup>56</sup>
NODAGA		RT, pH 4.0, 10 minutes, 3 μM	97 <sup>47</sup>
TRAP-OH	23.3 <sup>43</sup>	RT, pH 3.3, 5 minutes, 3 μM	88 <sup>30</sup>
TRAP-Ph	—	RT, pH 3.3, 5 minutes, 3 μM	80 <sup>30</sup>
TRAP-Pr	26.2 <sup>63</sup>	30 °C, pH 3, 5 minutes, 2.6 μM 60 °C, pH 1, 5 minutes, 2.6 μM	95 <sup>63</sup>
TRAP-(HMDA-DOTA) <sub>3</sub>	—	95 °C, pH 2, 5 minutes, 6.8 μM	97 <sup>66</sup>
NOPO	25.0 <sup>44,68</sup>	95 °C, pH 2.8, 5 minutes, 0.1 μM	100 <sup>44,68</sup>
NOPO-RGD	—	100 °C, pH 1.8, 5 minutes, 1 μM	94
MA-NOTMP	—	95 °C, pH 2.5, 5 minutes, 0.1 μM	100 <sup>72</sup>
PCTA-C-Bn-p-NO <sub>2</sub>	—	RT, pH 4–5, 5 minutes, 1 mM	98.9 <sup>57,58</sup>
Oxo-C-Bn-p-NO <sub>2</sub>	—	RT, pH 4–5, 5 minutes, 1 mM	98.5 <sup>57</sup>
(NH <sub>2</sub> ) <sub>2</sub> sar	—	85 °C, 30 minutes, 18 μM	100 <sup>69</sup>
L <sup>1</sup>	—	170 °C (150 W μwave), 7 minutes, 6.1 μM	69 <sup>23</sup>
L <sup>2</sup>	—	170 °C (150 W μwave), 7 minutes, 6.6 μM	49 <sup>23,73</sup>
L <sup>3</sup>	—	300 W μwave, 5 minutes, 0.1 mM	82 <sup>23</sup>
L <sup>4</sup>	—	300 W μwave, 5 minutes, 0.1 mM	83 <sup>23</sup>
L <sup>5</sup>	—	300 W μwave, 7 minutes, 0.1 mM	42 <sup>23</sup>
TeMP	—	100 °C, 45 minutes, 0.8 mM	90 <sup>74</sup>
TriMP <sup>N3</sup>	—	110 °C, 7 minutes, 0.06 mM	95 <sup>75</sup>
TriMP <sup>EG</sup>	—	110 °C, 7 minutes, 0.06 mM	95 <sup>75</sup>
TFPP	—	100 °C, pH 5.5, 60 minutes, 160 μM	99 <sup>76</sup>
NOTAM <sup>BP</sup>	—	95 °C, pH 4.2, 10 minutes, 21 μM	100 <sup>77</sup>
NO2AP <sup>BP</sup>	—	60 °C, pH 4.2, 10 minutes, 21 μM	100 <sup>77</sup>
TAFC	—	RT, pH 3.9, 15 minutes, 3 μM	100 <sup>78,80</sup>
FOX E	—	80 °C, 20 minutes	95 <sup>79,80</sup>
FSC	—	RT, pH 4, 15 minutes, 1 μM	95 <sup>81,82</sup>

The compound displayed high tumour uptake and low retention in organs, except for the excretion pathway through the kidneys.

Seeking to take advantage of the similarities of Ga(III) and Fe(III), Rösch and coworkers used a series of tetrapyrrole porphyrins to chelate <sup>68</sup>Ga.<sup>23</sup> Although radiolabelling using conventional heating methods was poor (<20%), microwave assisted radiolabelling of both water soluble and lipophilic tetrapyrroles was more successful, with yields greater than 80% being reported for two of the chelates tested after 5 minutes of radiolabelling.<sup>23</sup> Overall, the lipophilic tetrapyrroles L<sup>3</sup> and

L<sup>4</sup> showed greater radiolabelling and stability to transchelation and transmetallation, with >90% of the complex remaining intact after 2 hours in the presence of excess transferrin, than the hydrophilic L<sup>1</sup>. Indeed, in human serum L<sup>1</sup> was so unstable that it was indistinguishable from free <sup>68</sup>Ga – although this was suggested to be due to decomposition of the chelate in serum.<sup>23</sup> Preliminary imaging studies using L<sup>1</sup> in a rat model demonstrated the potential of these systems for targeting tumours – with a tumour to tissue ratio of 2 being achieved after allowing the system to equilibrate through tracer washout from the non-target tissues.<sup>23</sup>

Banerjee and coworkers recently demonstrated a highly stable <sup>68</sup>Ga-porphyrin system based on 5,10,15,20-tetra(4-methylpyridyl)porphyrin (TeMP).<sup>74</sup> Although high temperatures (100 °C) and ligand concentrations (0.8 mM) were required to achieve a 90% RCY, the resulting complex was stable to human serum, with 98% remaining intact after 2 hours.<sup>74</sup> Boyle and co-workers used a similar chelate, TriMP, which was functionalised with an azide group to conjugate the porphyrin to a peptide.<sup>75</sup> Again, microwave irradiation was used to promote chelation of <sup>68</sup>Ga by the porphyrin, with complexation being completed within 7 minutes when heated to 110 °C.<sup>75</sup> The polyfluorinated porphyrin, TFPP, was radiolabelled by Fazaeli and co-workers<sup>76</sup> – the resulting complex showed high stability, with 99% remaining after 5 hours under physiological conditions.<sup>76</sup> However, heating at 100 °C for 60 minutes was required for labelling of this system.<sup>76</sup>

A number of siderophores (Fig. 3), have been tested for their suitability as Ga(III) chelators. As Fe(III) binding compounds it can be expected that these chelators will also bind Ga(III) efficiently due to their similar properties (Table 2). After testing a panel of siderophores, Decristoforo and coworkers found that triacetylfusarin C (TAFC – Fig. 3) and ferrioxamine E (FOXE – Fig. 3) were the most suitable for application to gallium chelation.<sup>79,80</sup> While the majority of siderophores tested showed rapid gallium uptake under mild conditions, the resulting complexes formed by these two were highly stable (>95%) to a range of metabolic conditions – and most importantly survived *in vivo* when tested in rats.<sup>79,80</sup> Uptake was tested *in vitro* with a strain of fungi, *Aspergillus Fumigatus*, which lacked siderophore biosynthesis and as such relied on external siderophores as a source of iron.<sup>79,80</sup> Both FOXE and TAFC were taken up, as was Fusarin C (FSC – Fig. 3).<sup>79,80</sup> Later studies on Fusarin C demonstrated that it also rapidly chelated gallium and showed suitable stability to PBS, EDTA and human serum.<sup>81</sup> Decristoforo et al. noted that FSC was less stable to iron chloride transmetallation and DTPA transchelation than TAFC.<sup>78</sup> To assess the effect that acylation of the pendant amine of FSC had on the stability of the resultant complex, and to use this as a method of conjugating FSC to a targeting motif, they

tested two – FSC-(AcPro)<sub>3</sub> and FSC-(RGD)<sub>3</sub>.<sup>82</sup> Both derivatives could be rapidly labelled and showed high stability to human serum.<sup>82</sup>

Overall the improvements made in the field of cyclic chelators for <sup>68</sup>Ga are relatively mild – the promising TRAP and NOPO systems being comparable to NOTA for labelling efficiency, although the remote carboxylic functionalities of TRAP-Pr allow for easier conjugation of a targeting functionality. These chelates are however a significant improvement over the widely used DOTA for complexation of <sup>68</sup>Ga, in terms of complexation kinetics and the stability of the resulting complex. Ultimately, NOTA based chelates are still the superior cyclic chelates for <sup>68</sup>Ga – further work to improve upon the design of new chelates will be needed if NOTA is to be replaced.

2.2.2. Non-macrocyclic chelators. In recent years there has been a shift towards acyclic ligands for the chelation of <sup>68</sup>Ga. This movement away from macrocyclic chelates is due to the aims of rapid radiolabelling under mild conditions – room temperature and neutral pH – and at a low ligand concentration.

Developed by Orvig and coworkers, H<sub>2</sub>dedpa (Fig. 4) combines amine, pyridine and carboxylic acid functionalities to bind Ga(III) with a high stability.<sup>4</sup> The H<sub>2</sub>dedpa chelate and its derivatives rapidly coordinate <sup>68</sup>Ga, with quantitative radiochemical yields being reported at room temperature in 10 minutes.<sup>4</sup> This ligand shows high stability to transferrin over 2 hours, although functionalization of the amines results in a significant loss of stability.<sup>4,83</sup> Labelling of this chelate through the carbon backbone provides a route to conjugation without loss of stability – the C-c(RGDyK) conjugate complex was 92% stable to transferrin after 2 hours. The pyridine ring offers an alternative site for functionalization and manipulation of both this and the N-functionalisation site allowed for the lipophilicity of the resulting complex to be tailored.<sup>84</sup> The most lipophilic compounds showed greater stability to transchelation by transferrin<sup>84</sup> – Orvig et al. speculated this may be due to the polar nature of the transferrin binding site. The general biodistribution for this system is a rapid clearance from background tissue and excretion through kidneys. On the otherhand, the most functionalised derivatives were shown to accumulate in the liver due to their increased aromaticity.<sup>84</sup> RGD conjugates showed high tumour uptake but had slow blood clearance.<sup>4,84,85</sup>

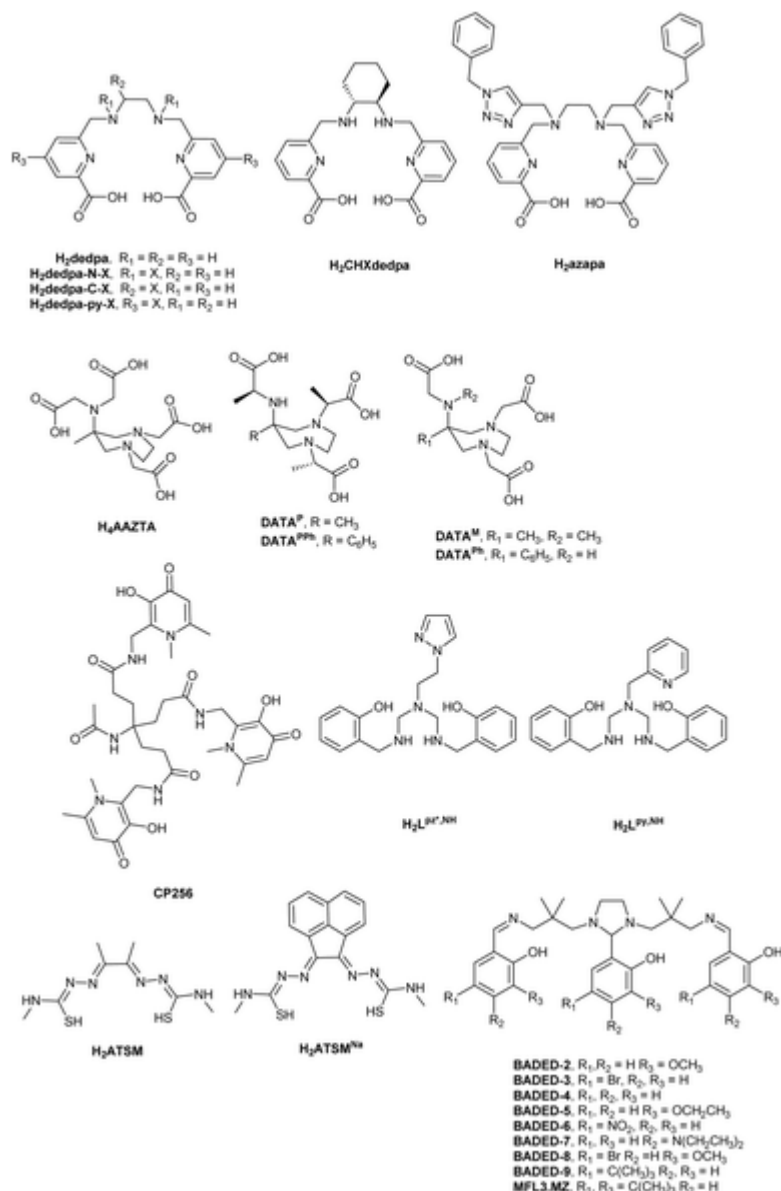


Fig. 4 Structures of novel non-macrocytic gallium chelators.

In contrast to other N-conjugates, a series of complexes conjugated to a nitroimidazole moiety showed relatively high stability to transferrin competition,<sup>22</sup> in addition to being suitable for hypoxia imaging. However, this series of chelates could only be labelled at ligand concentrations greater than  $10^{-4}$  M,<sup>22</sup> much higher than the unconjugated chelate which is reported to complex  $^{68}Ga$  at ligand concentrations as low as  $10^{-7}$  M.<sup>4</sup>

Although 99% stable to transferrin over 2 hours,<sup>4</sup> when tested for transmetallation in human serum the  $^{68}Ga$ -dedpa complex showed only 78% stability.<sup>86</sup> To improve the stability of the complex, the Orvig group increased the rigidity of the backbone by incorporating a cyclohexyl group.<sup>86</sup> The resulting  $^{68}Ga$ -CHXdedpa (Fig. 4) complex showed a 90% stability to human serum, although it showed a reduced radiolabelling at lower ligand concentrations.<sup>86</sup>  $H_2azapa$  (Fig. 4), designed to make

conjugation easier through a CuAAC “click” reaction, showed a reduced clearance in line with other N-functionalised H<sub>2</sub>dedpa complexes and only a 52% stability to transferrin over 2 hours.<sup>87</sup>

Originally used with manganese to create an MRI relaxation based contrast agent,<sup>88</sup> AAZTA (Fig. 4) has also been used for coordination of Ga(III).<sup>89–91</sup> Parker and coworkers showed that this system could be used to complex <sup>68</sup>Ga very rapidly under mild conditions. Forming a gallium complex with greater stability than Ga-transferrin, this system was applied in rats and showed only bladder and kidney uptake after 25 minutes.

Vologdin and coworkers applied Ga-AAZTA to a probe that could measure pH in vivo by combining MRI and PET properties.<sup>92</sup> The multimodal probe was constructed by conjugating a protected AAZTA chelate through an arylsulfonamide bridge to a protected DO3A moiety.<sup>92</sup> Selective deprotection of DO3A allowed for complexation of Gd(III) by the DO3A chelate; after deprotection of AAZTA the probe could be used to coordinate Ga(III) with the future potential for radiolabelling. The resultant Gd(III)-<sup>68</sup>Ga species would be used to measure pH due to the pH dependent relaxivity effect of gadolinium being quantifiable through the use of PET imaging to determine concentration, although radiolabelling of this complex has not yet been undertaken.

AAZTA was reported to form multiple complexes with Ga(III) by Parker et al.<sup>91</sup> This was speculated to be due to conformational changes in the seven membered ring. The formation of multiple complexes was still seen when DATA<sup>M</sup> (Fig. 4) was used as the chelator, despite its reduced number of coordination sites.<sup>91</sup> In contrast, increasing the steric hindrance to ring inversion by replacing a methyl group with a phenyl ring (DATA<sup>Ph</sup> and DATA<sup>PPh</sup>) resulted in a single complex being formed.<sup>90,91,93</sup> While the formation of <sup>68</sup>Ga-DATA complexes was slower than that of <sup>68</sup>Ga-AAZTA complexes,<sup>91</sup> the formation of a single complex is important for further characterisation of the system and wider acceptance of the ligand system. In addition, the additional products formed by AAZTA when complexing Ga(III) were less stable than the products of DATA chelation – the Ga(III)-DATA complexes were stable to DTPA, iron and transferrin over 2 hours,<sup>91</sup> and appeared to be biologically inert as activity was seen in only the kidneys and bladder of injected rats.<sup>91</sup> In a labelling study,<sup>94</sup> the DATA chelators have been reported to complex <sup>68</sup>Ga(III) across a range of conditions suitable for labelling – with a 97% yield at room temperature in 1 minute being achieved by 3.6 μM of chelator.<sup>94</sup>

A pair of N<sub>4</sub>O<sub>2</sub> chelators, H<sub>2</sub>L<sup>pz\*,NH</sup> and H<sub>2</sub>L<sup>py,NH</sup> (Fig. 4), were synthesised by Paulo and coworkers with either a pyridine or pyrazol arm.<sup>95</sup> The <sup>68</sup>Ga-L<sup>pz\*,NH</sup> complex showed poor stability, but the <sup>68</sup>Ga-L<sup>py,NH</sup> complex was stable to transferrin over 48

hours. This system showed fast blood clearance in mice and negligible bone uptake. Analysis of blood serum and urine samples confirmed that the  $^{68}\text{Ga}$  complex had not degraded in vivo. However, this system is hampered by the high temperatures (85 °C) required for complexation (Table 5).<sup>95</sup>

**Table 5** Stability and RCY of novel non-cyclic chelators for  $^{68}\text{Ga}$

Chelator	Log $K_{\text{Ga-L}}$	Labelling conditions	RCY/%
H <sub>2</sub> dedpa	28.11 <sup>4</sup>	RT, pH 4.5, 10 minutes, 0.1 μM	95 <sup>5</sup>
H <sub>2</sub> CHXdedpa	27.61 <sup>86</sup>	RT, pH 4, 10 minutes, 10 μM	99 <sup>86</sup>
H <sub>4</sub> AAZTA	22.2 <sup>89,90</sup>	RT, pH 4, 1 minute, 1 μM	97 <sup>91</sup>
H <sub>3</sub> DATA <sup>M</sup>	—	RT, pH 5, 5 minutes, 3.6 μM	98 <sup>94</sup>
H <sub>3</sub> DATA <sup>P</sup>	—	RT, pH 5, 5 minutes, 3.6 μM	96 <sup>94</sup>
H <sub>3</sub> DATA <sup>Ph</sup>	—	RT, pH 5, 5 minutes, 5 μM	99 <sup>94</sup>
H <sub>3</sub> DATA <sup>PPH</sup>	—	RT, pH 7, 15 minutes, 3.6 μM	98 <sup>94</sup>
H <sub>2</sub> L <sup>pz*,NH</sup>	—	85 °C, pH 5, 15 minutes, 1 mM	25 <sup>95</sup>
H <sub>2</sub> L <sup>py,NH</sup>	—	85 °C, pH 5, 15 minutes, 60 μM	95 <sup>95</sup>
CP256	—	RT, pH 6.5, 5 minutes, 10 μM	98 <sup>45</sup>
H <sub>2</sub> ATSM <sup>Na</sup>	—	90 °C, 30 minutes, 200 μM	70 <sup>97</sup>
BADED-2	—	80 °C, pH 4.3, 10 minutes, 40 μM	97 <sup>98</sup>
BADED-3	—	80 °C, pH 4.3, 10 minutes, 30 μM	98 <sup>98,99</sup>
BADED-4	—	80 °C, pH 4.3, 10 minutes, 50 μM	98 <sup>98,99</sup>
BADED-5	—	80 °C, pH 4.3, 10 minutes, 40 μM	97 <sup>98,99</sup>
BADED-6	—	80 °C, pH 4.3, 10 minutes, 40 μM	98 <sup>98</sup>
BADED-7	—	80 °C, pH 4.3, 10 minutes, 30 μM	97 <sup>98</sup>
BADED-8	—	80 °C, pH 4.3, 10 minutes, 30 μM	98 <sup>98,99</sup>
BADED-9	—	80 °C, pH 4.3, 10 minutes, 30 μM	98 <sup>98,99</sup>
MFL3.MZ	—	80 °C, pH 4.3, 10 minutes, 80 μM	55 <sup>99</sup>

Originally an iron chelator, CP256 (Fig. 4), which utilises hydroxypyridone units to chelate  $^{68}\text{Ga}$  was shown to have promising properties.<sup>45</sup> This chelate bound  $^{68}\text{Ga}$  rapidly under mild conditions – near quantitative yields were achieved in 10 minutes at room temperature and pH 6.5 with only 10 μM of ligand.<sup>45</sup> This matches well with the performance of NOTA, and at lower chelate concentrations CP256 outperforms NOTA – with a RCY approximately double that of NOTA at 1 μM.<sup>45</sup> This rapid radiolabelling is accompanied by a high kinetic stability –  $^{68}\text{Ga}$ -CP256 showed significant stability to transferrin with no transchelation seen after 4 hours incubation.<sup>45</sup> Conjugation to the protein C2Ac was achieved through a maleimide derivative of CP256.<sup>45</sup> This protein conjugate retained the in vitro calcium binding properties of the parent protein, and in a small mammal

study the complex was found only in excretory organs<sup>45</sup> supporting the high stability previously seen. Two isothiocyanate containing derivatives have also been developed, conjugation through the isothiocyanate functionality to c(RGDfK) resulted in a probe that showed high stability in vivo with no bone uptake being observed and a receptor dependent tumour uptake being displayed.<sup>96</sup>

Dilworth et al.<sup>97</sup> applied the thiosemicarbazone, H<sub>2</sub>ATSM (Fig. 4), to <sup>68</sup>Ga chelation with limited success – the resulting complex was poorly soluble in water and highly unstable in foetal bovine serum. This instability is likely due to the partial coordination of gallium by the four coordinate ligand – the complex that forms includes a chloride ion coordinated to the Ga(III) centre. Adaptation of the chelate to incorporate a naphthalene backbone (Fig. 4), increased stability significantly, although degradation from the chloride complex to the hydroxide complex was seen over time.<sup>97</sup> This hydroxide complex led to cleavage of one of the thiosemicarbazone arms. The H<sub>2</sub>ATSM<sup>Nap</sup> ligand was not isolated – however the zinc complex could be. Displacement of the zinc ion by <sup>68</sup>Ga was used for radiolabelling in ethanol, achieving a 70% yield after 30 minutes reaction at 90 °C.<sup>97</sup>

Rösch and coworkers applied a range of Schiff ligands with the BADED backbone to the complexation of <sup>68</sup>Ga(III).<sup>98,99</sup> All ligands were able to rapidly complex <sup>68</sup>Ga at elevated temperatures except for the most sterically hindered ligand MFL3.MZ.<sup>99</sup>

The field of acyclic <sup>68</sup>Ga chelators has developed significantly in recent years – a number of new, highly promising chelators that are comparable to NOTA in terms of radiolabelling kinetics and kinetic inertness of the resulting complex have been reported. The AAZTA<sup>89,91</sup> and DATA<sup>94</sup> families of chelates show extremely rapid complexation at room temperature (1 minute and 3 minutes respectively) – although this system has not yet been tested for its radiolabelling efficiency after conjugation to a targeting probe.

The importance of selecting the conjugation site carefully was highlighted by Orvig et al. and their work with the H<sub>2</sub>dedpa chelator – chelation through one of the amine binding sites had unpredictable consequences for the stability of the resulting complex.<sup>4,100</sup> Circumventing this by implementing an alternate, easily accessible, chelation site may see the H<sub>2</sub>dedpa system becoming more widely adopted. The impressive CP256 chelator<sup>45</sup> shows extremely high stability to transchelation by transferrin and initial studies in vivo are promising.

### 2.3. Gallium conclusions

The work undertaken in recent years has moved gallium chelates much closer to widespread use. The acceptance and application of <sup>68</sup>Ga-DOTA derivatives to

medical studies is promising and demonstrates the value of this isotope as a diagnostic tool.<sup>51–55</sup>

The increased affinity seen for  $^{68}\text{Ga}$ -TRAP-(RGD)<sub>3</sub><sup>64</sup> when compared to  $^{68}\text{Ga}$ -DOTA-RGD is promising for the future of this system – if this increase in affinity is transferable to other bioconjugates then the use of TRAP chelates instead of DOTA chelates would be highly favourable. The separation of conjugation functionality from the binding core also makes it easier to create a variety of different tracers with specific applications without increasing transchelation.

The acyclic chelates AAZTA<sup>91</sup> and CP256<sup>45</sup> are both highly promising for future development. While AAZTA appears to form multiple complexes,<sup>91</sup> the DATA derivatives eliminate this problem whilst retaining the rapid (<3 minute) complexation of  $^{68}\text{Ga}$ .<sup>94</sup> CP256 has displayed very impressive gallium complex stability to transferrin alongside rapid  $^{68}\text{Ga}$  complexation at low concentrations of ligand.<sup>45</sup> Further development of these two ligand systems will highlight the value of acyclic chelators in the future of  $^{68}\text{Ga}$  PET.

The use of preformed coordinating centers appears to be key to the production of an inert metal-chelate complex as shown by the kinetic stability of NOTA, tetrapyrrole and DATA complexes, and the improved stability of the more rigid  $^{68}\text{Ga}$ -CHXdedpa complex in comparison to the complex formed from the linear H<sub>2</sub>dedpa system in human serum. The use of a preformed coordinating face in the DATA ligands offers an inert alternative to the macrocyclic systems, such as NOTA, that can withstand transferrin competition and also rapidly complex  $^{68}\text{Ga}$ . Incorporation of this style of preformed core into future chelates may allow for improved retention of  $^{68}\text{Ga}$  in vivo without negatively impacting upon radiolabelling kinetics.

Interestingly, CP256 and H<sub>2</sub>L<sup>py,NH</sup>, which do not have a rigid preformed structure, also display high inertness to transferrin competition. This may be due to the branched nature of these chelates, rather than linear, resulting in reduced degrees of freedom and therefore less entropic drive to decomplexation.

### 3. Chelating copper-64

A number of copper isotopes emit positrons;  $^{64}\text{Cu}$  ( $t_{1/2} = 12.7$  hours) has the second longest half-life of the metal based PET isotopes.<sup>9</sup> This is significantly longer than the traditional PET isotopes  $^{11}\text{C}$  (20 minutes) and  $^{18}\text{F}$  (109 minutes). As such  $^{64}\text{Cu}$  has the potential to be applied to targeting motifs that have a longer blood lifetime such as antibodies.<sup>101</sup>

$^{64}\text{Cu}$  is produced in a cyclotron by bombarding an enriched nickel target ( $^{64}\text{Ni}(\text{d}, 2\text{n})^{64}\text{Cu}$  or  $^{64}\text{Ni}(\text{p}, \text{n})^{64}\text{Cu}$ ).<sup>102</sup>  $\text{Cu}(\text{II})$  can form stable complexes with coordination numbers from 4 to 6.<sup>8</sup> The resulting complexes have varied geometries due to the variation in coordination number, those with a coordination number of 6 typically having an octahedral geometry which may undergo Jahn–Teller distortion. Under physiological conditions,  $\text{Cu}(\text{II})$  can be reduced to  $\text{Cu}(\text{I})$  – this has the potential to cause demetallation of the complex. As such, it is important for a chelator selected for use with  $^{64}\text{Cu}$  to be able to complex both  $\text{Cu}(\text{I})$  and  $\text{Cu}(\text{II})$  or to stabilise  $\text{Cu}(\text{II})$  to prevent reduction. This property of copper can be exploited for imaging of hypoxia as demonstrated by Dearling and coworkers.<sup>103</sup> Whilst the reductive potential of a complex can be used as a measure of the potential in vivo stability, little has been done to design chelates specifically based on this property. As a result, and due to the poor translation of this property across the metals investigated, the reductive potential has not been extensively explored in this review.

Copper is the third most abundant trace metal in the body, after iron and zinc.<sup>21</sup> As such, a number of proteins incorporate copper<sup>104</sup> and could potentially compete with a chelate to bind  $^{64}\text{Cu}$ .  $\text{Cu}(\text{II})$  ions administered directly into the blood stream, by I.V. or orally, are initially bound by albumin, a copper transport protein.<sup>15</sup> This leads to rapid clearance of  $^{64}\text{Cu}$  from the blood<sup>105</sup> to the liver.<sup>15</sup> Ceruloplasmin accounts for 65–70% of the copper in human serum.<sup>104</sup>  $^{64}\text{Cu}$  deposited in the liver by albumin is incorporated into ceruloplasmin and then returns to the bloodstream<sup>15</sup> where it is slowly transferred to other organs.<sup>21</sup>

### 3.1. First generation $^{64}\text{Cu}$ chelators

Macrocycles were shown to be more stable chelators of copper than their acyclic counterparts in 1969 when Cabbiness et al. compared 5,7,7,12,14,14-hexamethyl-1,4,8,11-tetraazacyclotetradecane (tet-a – Fig. 5) and  $\text{N,N}'$ -di(2-aminoethyl)-propylenediamine.<sup>106</sup> While both ligands share the same coordination sites and spacing, the macrocycle tet-a forms a much more stable complex when binding to copper. Accordingly, the majority of chelates studied for the binding of  $^{64}\text{Cu}$  have been macrocyclic in nature.

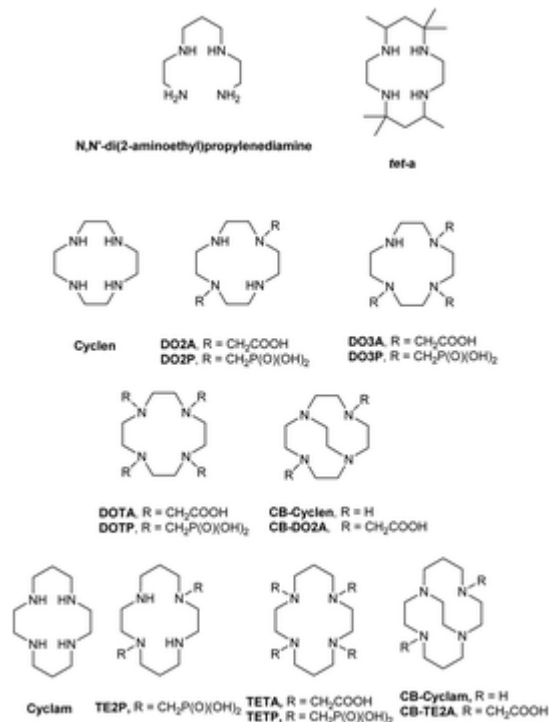


**Fig. 5** Structure of copper chelators.

A comparison of the stability of three common macrocyclic chelates in radiochemistry, NOTA, DOTA and TETA (Fig. 3) suggests that DOTA provides the optimum stability for a copper complex due to its highest stability constant (21.63,<sup>107</sup> 22.63 (ref. 108) and 20.49 (ref. 109) respectively). However a comparison of the half-life of the Cu-DOTA and Cu-TETA complexes under acidic conditions suggests a greater stability for TETA under these conditions (Table 6).<sup>110</sup> Interestingly, 1,4,8,11-tetraazacyclotetradecane (cyclam – Fig. 5) has a much higher stability constant<sup>114</sup> than TETA, despite having fewer coordination sites – however a comparison of the stability of these complexes in acidic conditions again reveals Cu(II)-TETA to have a greater stability.<sup>110</sup>

**Table 6** Stability of copper-chelate complexes and radiolabelling conditions

Chelator	Log K <sub>Cu-L</sub>	Acid half-life	Labelling conditions	RCY
tet-a	28.0 <sup>106</sup>	1.1 hours (5 M HCl, 90 °C) <sup>110</sup>		
N,N'-Di(2-aminoethyl)propylenediamine	23.9 <sup>111</sup>			
EDTA	18.9 <sup>107</sup>			
NOTA	21.63 <sup>107</sup>	<3 minutes (5 M HCl, 30 °C) <sup>8</sup>		

Chelator	Log K <sub>Cu-L</sub>	Acid half-life	Labelling conditions	RCY
Cyclen	24.60 <sup>112</sup>	9.53 minutes (5 M HClO <sub>4</sub> , 25 °C) <sup>112</sup>		
DO2A	18.9 <sup>108</sup>		RT, pH 5.5, 120 minutes, 5 mM	100 <sup>108</sup>
DO3A	22.87 <sup>113</sup>			
DOTA	22.63 <sup>108</sup>	<1 minute (5 M HCl, 90 °C) <sup>110</sup> 28.1 h (5 M HClO <sub>4</sub> , 25 °C) <sup>112</sup>	RT, pH 5.5, 120 minutes, 5 mM	99 <sup>108</sup>
DO2P	28.7 <sup>108</sup>		90 °C, pH 6.5, 4 hours, 2 mM	97.8 <sup>108</sup>
DO3P	26.9 <sup>108</sup>		RT, pH 6.5, 120 minutes, 2 mM	96.6 <sup>108</sup>
DOTP	26.2 <sup>108</sup>		RT, pH 6.5, 120 minutes, 2 mM	96.9 <sup>108</sup>
CB-DO2A		<2 minutes (5 M HCl, 30 °C) <sup>110</sup>		
Cyclam	27.2 <sup>114</sup>	2.7 days (5 M HCl, 30 °C) <sup>110</sup>		
CB-Cyclam	27.1 <sup>114</sup>	18.5 days (5 M HCl, 30 °C) <sup>110</sup>	75 °C, (4.7% 1 N NaOH/EtOH), 60 minutes, 10 mM	99 <sup>114</sup>
TETA	20.49 <sup>109</sup>	3.5 days (5 M HCl, 30 °C) <sup>110</sup>		
TE2P	26.5 <sup>109</sup>	6.7 months (5 M HClO <sub>4</sub> , 25 °C)		
TETP	26.6 <sup>115</sup>			
CB-TE2A		154 hours (5 M HCl, 90 °C) <sup>110</sup>	95 °C, pH 8.0, 2 hours, 10 μM	95 <sup>116</sup>

The incorporation of an ethylene cross bridge into the cyclam ring results in a drastic increase in stability of the resultant copper complex. The 1,4,8,11-

tetraazabicyclo[6.6.2]hexadecane (CB-cyclam – Fig. 5) copper complex has a half-life in acidic media six times longer than cyclam (Table 6),<sup>114</sup> and the 1,4,8,11-tetraazabicyclo[6.6.2]hexadecane-1,8-biacetic acid (CB-TE2A – Fig. 5) copper complex has a half-life over two thousand times longer than TETA (Table 6).<sup>114</sup> The same is not true for 1,4,7,10-tetraazabicyclo[5.5.2]dodecane-1,7-biacetic acid (CB-DO2A – Fig. 5) which forms a less stable complex than DOTA (Table 6).<sup>114</sup>

To investigate the effect of an overall negative charge on the biodistribution of macrocyclic complexes, Sun et al. synthesised and tested a range of cyclen derivatives with phosphonic acid pendant arms to compare to the previously tested carboxylic acid based chelates.<sup>108</sup> Methylphosphonic acid derivatives of cyclen (Fig. 5) showed an increased stability when compared to the equivalent acetic acid chelates for the coordination of copper ( $\log K_{\text{Cu-DOTA}} = 22.63$ ,  $\log K_{\text{Cu-DOTP}} = 26.2$ ,  $\log K_{\text{Cu-DO3A}} = 22.87$ ,  $\log K_{\text{Cu-DO3P}} = 26.9$ ,  $\log K_{\text{Cu-DO2A}} = 18.9$ ,  $\log K_{\text{Cu-DO2P}} = 18.7$ ).<sup>113,114</sup> These phosphonic acid containing complexes also showed high bone uptake making them potential bone-targeting imaging agents.<sup>108</sup> Increased stability was also seen for TETP (1,3,8,11-tetraazacyclotetradecane-N,N',N'',N'''-tetra(methylphosphonic acid) – Fig. 5 –  $\log K_{\text{Cu-TETP}} = 26.6$ )<sup>115</sup> in comparison to TETA ( $\log K_{\text{Cu-TETA}} = 20.49$ ).<sup>109</sup>

### 3.2. Current developments in copper chelate design

3.2.1. Macrocyclic <sup>64</sup>Cu chelators. Due to the stability of CB-TE2A in comparison to TETA, a number of cyclam derivatives with different crossbridge motifs have recently been investigated. One of the most significant incorporates a propylene cross bridge instead of an ethylene cross bridge to form PCB-TE2A (Fig. 6).<sup>119</sup> The Cu-PCB-TE2A complex displays remarkable stability under acidic conditions; it is reported that no degradation was seen after seven days in 12 M HCl at 90 °C. This is superior to CB-TE2A which has a half-life of 6.4 days in 5 M HCl at 90 °C.<sup>110</sup> Radiolabelling of PCB-TE2A also proceeded faster and at a lower temperature than that of CB-TE2A (Table 7).<sup>116</sup> The <sup>64</sup>Cu-PCB-TE2A complex showed no signs of decomplexation after 24 hours in rat serum at 37 °C, and showed rapid clearance when tested in rats.<sup>119</sup> Extension of the cross-bridging link also significantly improved the kinetic stability of CB-DO2A; in 2011, Anderson and coworkers applied a propyl cross-bridged DO2A ligand, C3B-DO2A, to the complexation of Cu(II).<sup>124</sup> Although this ligand required microwave heating under acidic conditions to promote complexation, the resulting complex, <sup>64</sup>Cu-C3B-DO2A, showed much higher kinetic stability ( $t_{1/2} = 1.1$  days, 12 M HCl, 90 °C)<sup>124</sup> to acid promoted decomplexation than the ethyl cross-bridged analogue CB-DO2A ( $t_{1/2} = <2$  minutes, 5 M HCl, 30 °C).<sup>110</sup>

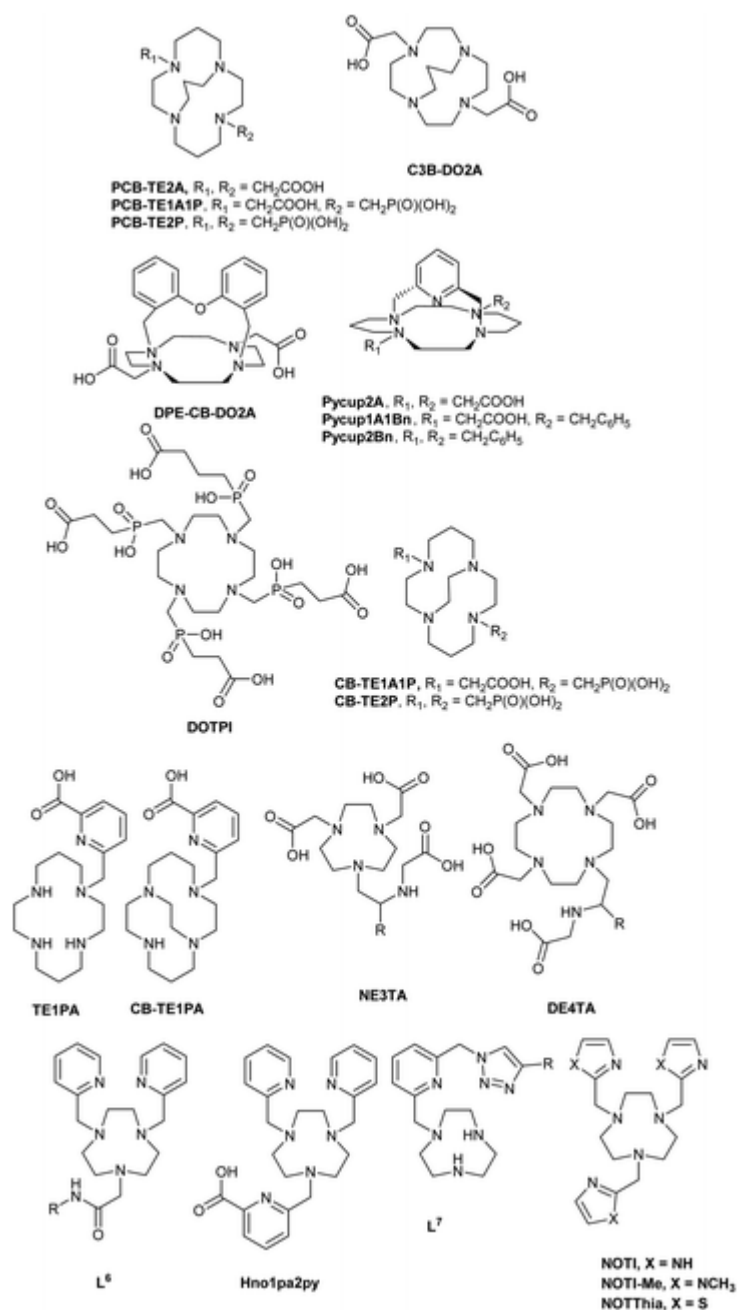


Fig. 6 Structures of new copper macrocyclic chelators.

Table 7 Stability and radiolabelling conditions of novel copper-chelate complexes

Chelator	Log $K_{\text{Cu-L}}$	Acid half-life	Labelling conditions	RCY
Pycup2A		2.7 hours (5 M HCl, 90 °C) <sup>117</sup>	70 °C, pH 7.4, 15 minutes, 10 μM	100 <sup>117</sup>
Pycup1A1Bn		1.5 hours (5 M HCl, 90 °C) <sup>117</sup>	70 °C, pH 7.4, 15 minutes, 10 μM	100 <sup>117</sup>
Pycup2Bn		20.3 hours (5 M HCl, 90 °C) <sup>117</sup>	70 °C, pH 7.4, 15 minutes, 10 μM	100 <sup>117</sup>
DOTPI	23.1 <sup>118</sup>		20 °C, pH 3, 5 minutes, 10 μM	90 <sup>118</sup>
PCB-TE2A		>7 days (12 M HCl, 90 °C) <sup>119</sup>	70 °C, pH 8, 60 minutes, 5 mM	100 <sup>119</sup>
TRAP <sup>Pr</sup>	19.1 <sup>65</sup>	2 hours (pH 3.5, 25 °C) <sup>65</sup>	25 °C, pH 3, 5 minutes, 1 μM	100 <sup>120</sup>

Chelator	Log K <sub>Cu-L</sub>	Acid half-life	Labelling conditions	RCY
NOPO			25 °C, pH 3, 5 minutes, 1 μM	100 <sup>120</sup>
CBTE2P		3.8 hours (5 M HCl, 90 °C) <sup>121</sup>	RT, pH 8.1, 30 minutes, 26.5 μM	>95 <sup>121</sup>
CBTE1A1P		6.8 hours (5 M HCl, 90 °C) <sup>121</sup>	RT, pH 8.1, 30 minutes, 26.5 μM	>95 <sup>121</sup>
PCB-TE1A1P		8 days (12 M HCl, 90 °C) <sup>122</sup>	60 °C, pH 8, 1 hour, 25 μM	95 <sup>122</sup>
PCBTE2P		>2 days (5 M HCl, 90 °C) <sup>123</sup>	90 °C, pH 8, 10 minutes, 5 mM	100 <sup>123</sup>
C3B-DO2A		1.1 day (12 M HCl, 90 °C) <sup>124</sup>	100 °C (μwave), pH 3, 2 hours, 47 μM	97 <sup>124</sup>
TE1PA	25.5 <sup>125</sup>	32 minutes (1 M HCl, 25 °C) <sup>125</sup>	RT, 15 minutes, 10 μM	99 <sup>126</sup>
NE3TA			RT, pH 5.5, 1 minute, 1 mM	99.9 <sup>127</sup>
DE4TA			RT, pH 5.5, 1 minute, 1 mM	99.6 <sup>127</sup>
L <sup>6</sup>			RT, pH 5.5, 30 minutes, 30 μM	99 <sup>128</sup>
Hno1pa2py	20.96	204 minutes (3 M HCl, 90 °C)	RT, pH 6.5, 30 minutes, 0.1 mM	25 <sup>129</sup>
L <sup>7</sup>			RT, pH 5.5, <5 minutes, 0.1 mM	100 <sup>130</sup>
NOTI		30 seconds (5 M HCl, RT)	RT, pH 7.4, <1 minute, 1 μM	>95 <sup>131</sup>
NOTI-Me		30 seconds (5 M HCl, RT)	RT, pH 7.4, <1 minute, 1 μM	>95 <sup>131</sup>
NOTThia		55 hours (5 M HCl, 95°)	RT, pH 7.4, <1 minute, 1 μM	>95 <sup>131</sup>

Incorporation of a heteroatom, in the form of diphenylether, into the cross bridge of cyclen derivatives also results in an increase in stability to acid. The resulting Cu-DPECB-DO2A (Fig. 6) complex has a half-life of 30.8 days in 12 M HCl at 90 °C,<sup>132</sup> however radiolabelling has not yet been carried out on this complex. This shows a significantly higher stability to acid catalysed decomplexation when compared to CB-DO2A which degraded in less than 2 minutes under much milder conditions.<sup>110</sup> Inspired by this improvement in stability, the pycup ligand, a pyridine cross-bridged cyclam ligand, (Fig. 6) was assessed for its suitability in <sup>64</sup>Cu chelation.<sup>117</sup> The incorporation of pyridine into the cross bridge could potentially reduce the need for additional coordination sites – this would allow for conjugation to one of the pendant carboxylate arms without interfering with coordination the metal. Assessment of the acid half-life of Cu-pycup complexes with a varying number of acidic arms showed that these arms were not needed for a high stability – pycup2A which incorporated two acetic acid arms had a half-life of only 2.7 hours in 5 M HCl at 90 °C whereas pycup2Bn had a half-life of 20.3 hours under these conditions.<sup>117</sup> All pycup derivatives tested showed high stability in rat plasma, and when tested in vivo showed rapid renal clearance and low uptake in

non-target organs.<sup>117</sup> Whilst complexation at low pH was poor, quantitative yield was found at 70 °C in 15 minutes at pH 7.4.<sup>117</sup> From these studies it is apparent that modification of the cross bridge can be a powerful tool to improve the stability<sup>119</sup> or the radiolabelling conditions<sup>117</sup> of the resultant copper complex.

The TRAP and NOPO ligands (Fig. 3) have been labelled with <sup>64</sup>Cu by Simecek et al.<sup>120</sup> These chelates rapidly form copper complexes and, although they were vulnerable to transchelation by EDTA, the chelate-copper complexes showed good stability in human plasma for over 12 hours.<sup>120</sup> TRAP(CHX)<sub>3</sub> (t<sub>1/2</sub> = 10 h – pH 3.5, 25 °C)<sup>65</sup> was shown to be more kinetically stable than TRAP-Pr (t<sub>1/2</sub> = 2 h – pH 3.5, 25 °C).<sup>65</sup> However in a stability study comparing TRAP(RGD)<sub>3</sub>, NOPO-RGD and NODAGA-RGD, NODAGA (Fig. 3) was shown to be more stable than either TRAP or NOPO with less than 5% transchelation over 12 hours in either EDTA or human plasma.<sup>120</sup> In 0.1 M EDTA, both TRAP(RGD)<sub>3</sub> and NOPO-RGD had more than 10% decomplexation over 12 hours. From this it is evident that the NOTA core forms a more stable copper complex than the TRAP core.

TE1PA (Fig. 6) is a cyclam based ligand with a single picolinic acid pendant arm. This ligand can bind <sup>64</sup>Cu(II) very rapidly,<sup>126</sup> however the resulting complex is vulnerable to acidic conditions with a half-life of 32 minutes in 1 M HCl.<sup>125</sup> In comparison, Cu-cyclam has a half-life of 2.7 days in 5 M HCl despite having no pendant arms.<sup>114</sup> A cross – bridged analogue, CB-TE1PA, has a significantly improved kinetic stability, with a half-life of 7.8 hours in 5 M HCl.<sup>133</sup> This cross-bridged derivative has not yet been reported to have been radiolabelled, but the improvement in stability is promising for future development.

Modification of cyclen with pendant phosphonic acid groups was undertaken by Simecek et al. in 2013<sup>118</sup> to form the 1,4,7,10-tetraazacyclododecane-1,4,7,10-tetrakis(methyl(2-carboxyethyl)phosphonic acid) (DOTPI – Fig. 5) chelate. While this chelate did not form a stable complex with Ga(III) (in contrast to TRAP),<sup>41</sup> DOTPI readily formed a Cu(II) complex.<sup>118</sup> The RGD conjugated chelate was radiolabelled with <sup>64</sup>Cu and the resulting complex showed a high stability to EDTA and human plasma (99% remaining complexed after 12 h) and a high affinity for the α<sub>v</sub>β<sub>3</sub> integrin (IC<sub>50</sub> = 73 pM, c(RGDyK) IC<sub>50</sub> = 1330 pM).<sup>118</sup>

Anderson and coworkers applied phosphonate pendant arms to CB-TE2A to form CBTE2P<sup>134</sup> (Fig. 5) and CBTE1A1P<sup>121</sup> (Fig. 5) with a view to overcoming the poor labelling kinetics of CB-TE2A whilst retaining the high stability of the resulting complex. This adaptation resulted in a significant improvement in radiolabelling, with 95% labelling at room temperature in 30 minutes. In contrast, CB-TE2A showed negligible labelling under the same conditions.<sup>121</sup> Although some loss in in vitro stability compared to Cu-CB-TE2A was reported,<sup>121</sup> Cu-CB-TE2P and Cu-CB-

TE1A1P both had half-lives greater than 3.5 hours in 5 M HCl at 90 °C.<sup>121</sup> Due to their rapid clearance from the liver, the in vivo stability of <sup>64</sup>Cu-CB-TE2P and <sup>64</sup>Cu-CB-TE1A1P was reported to be high<sup>121</sup> and this has been supported by further investigations of these systems using bioconjugated derivatives such as CB-TE1K1P.<sup>135,136</sup>

A number of derivatives of triazacyclononane (tacn) have recently been applied to the complexation of <sup>64</sup>Cu. Wu and coworkers demonstrated rapid chelation of <sup>64</sup>Cu with a range of bifunctional macrocyclic chelators including NE3TA and DE4TA.<sup>127</sup> These chelates were successfully radiolabelled to >99.5% in less than 1 minute at room temperature. NE3TA and DE4TA copper complexes showed high stability in human serum, with no decomplexation being seen over 48 hours. However, DE4TA was vulnerable to transmetallation by EDTA, with 44% of the complex being degraded over 24 hours. This instability was also seen in vivo with 11.1% of the injected dose of <sup>64</sup>Cu-DE4TA being retained in the liver after 24 hours and 5.7% in the kidneys. In contrast, <sup>64</sup>Cu-NE3TA showed <0.2% injected dose per gram in all organs and blood 24 hours post-injection indicating good stability in vivo.<sup>127</sup>

A recent trend has been the incorporation of heterocyclic arms to increase the coordination number of tacn. Bergmann and coworkers investigated a tacn derivative with two methylpridine arms and an acetic acid arm (L<sup>6</sup>) that was used to conjugate to a peptide through an amide bond. The resulting peptide conjugate was radiolabelled to >99% at 25 °C in 30 minutes.<sup>128</sup> However, this complex showed poor stability in human blood; only 40% of the complex remained intact after 4 hours when a specific activity of 10 MBq μg<sup>-1</sup> was used. When a lower specific activity (1 MBq μg<sup>-1</sup>) was used the stability in human blood was much greater – with 96% of the complex remaining intact after 24 hours in contrast to just 2.4% at higher activities.<sup>128</sup> It was speculated by Bergmann and coworkers that this was due to saturation of the proteins that cleaved the peptide, however this may also lead to saturation of the desired receptor in vivo. 60 minutes after injection a low liver and kidney activity was reported, with 3.5% retention in the kidneys and 1.2% in the liver of rats.<sup>128</sup> Roger and coworkers developed a similar ligand, Hno1pa2py, with a methylpicolinic acid arm in place of acetic acid.<sup>129</sup> This ligand can complex 100% of the <sup>64</sup>Cu present in solution after 30 minutes at room temperature and neutral pH in ammonium acetate buffer. However, only 25% of the activity can be assigned to the expected complex using radio-HPLC with the remaining activity being due to two other species. HPLC analysis of the cold complexation mixture showed the formation of two species – possibly due to the 7 potential coordination sites of the ligand resulting in different conformations of the resulting complex as Cu(II) will typically only accept 6 donors.<sup>129</sup> Interestingly, the majority of the activity after radiolabelling with <sup>64</sup>Cu (60%) was due to a species

not seen in the cold experiment. This may be due to the relatively low copper concentration under radiolabelling conditions, or due to the formation of hydroxyl radicals by radiolysis which would not be present during “cold” complexation (Table 8).<sup>129</sup>

**Table 8** Stability and RCY for non-macrocylic <sup>64</sup>Cu chelators

Chelator	Log K <sub>Cu-L</sub>	Acid half-life	Labelling conditions	RCY
H <sub>2</sub> dedpa	19.16 <sup>83</sup>	<5 minutes (6 M HCl, 90 °C) <sup>83</sup>	RT, pH 5.5, 10 minutes, 10 μM	99 <sup>83</sup>
H <sub>2</sub> azapa			RT, pH 5, 10 minutes, 182 mM	99 <sup>87</sup>
L <sup>8</sup>	16.56 <sup>137</sup>		RT, pH 5.5, 1 minute, 0.2 μM	100 <sup>138</sup>
L <sup>9</sup>			RT, pH 5.5, 1 minute, 0.2 μM	100 <sup>138</sup>
L <sup>10</sup>	18.31 <sup>137</sup>		RT, pH 5.5, 1 minute, 0.2 μM	100 <sup>138</sup>
L <sup>11</sup>			RT, pH 5.5, 1 minute, 0.2 μM	100 <sup>138</sup>
L <sup>12</sup>			RT, pH 5.5, 1 minute, 0.2 μM	100 <sup>138</sup>
L <sup>13</sup>			RT, pH 5.5, 1 minute, 0.2 μM	100 <sup>138</sup>
L <sup>14</sup>			50 °C, pH 5.5, 30 minutes, 2 mM	94 <sup>139</sup>
L <sup>15</sup>			50 °C, pH 5.5, 30 minutes, 2 mM	93 <sup>139</sup>
L <sup>16</sup>			50 °C, pH 5.5, 30 minutes, 2 mM	96 <sup>139</sup>

Viehweger and coworkers used “click” chemistry to conjugate a pyridyl functionalised tacn unit to a peptide (L<sup>7</sup>);<sup>130</sup> this route was selected to simplify the conjugation procedure and to remove the need for protection and deprotection during this step. Whilst the chelate required less than 5 minutes to achieve 100% radiolabelling, the peptide conjugate was 100% labelled in 30 minutes.<sup>130</sup> After 24 hours in the presence of a 20 fold excess of TETA, >95% of the radiolabelled complex remained. The radiolabelled peptide conjugate was quite stable to human serum – with only 6% <sup>64</sup>Cu decomplexed over 2 hours at 37 °C and 16% over 24 hours.<sup>130</sup>

Gotzmann and coworkers incorporated imidazole and thioimidazole arms into tacn to develop a rapid chelator for copper-64.<sup>131</sup> These arms were selected due to the complex formation constants of the free imidazole with copper in contrast to that of acetic acid – imidazole has a log β<sub>1</sub> = 4.21 whereas acetic acid has log β<sub>1</sub> = 1.79, this indicates that a tacn ligand incorporating imidazole arms will have more favourable complex formation than NOTA. Of the three ligands tested by Gotzmann and coworkers, NOTThia, which incorporates thiazole arms, was the best. All three ligands showed very rapid complexation at room temperature and a range of pH values<sup>131</sup> and showed a high stability to transmetallation with natural abundance copper (<2% decomplexation of <sup>64</sup>Cu over 24 hours in the presence of

5-fold natural abundance copper).<sup>131</sup> When assessed in human serum, each ligand showed some instability with approximately 10% decomplexation occurring over 24 hours. NOTThia outperformed the two imidazole based ligands when exposed to 5 M hydrochloric acid – the thiazole complex had a half-life of 55 hours at 95 °C whereas the two imidazole based ligands had half-lives of 30 seconds at room temperature.<sup>131</sup> This is likely due to the low pK<sub>a</sub> of thiazole (2.80) in comparison to the imidazole units (7.00–7.10) resulting in less protonation of the thiazole at low pH values and therefore a more stable complex. All three <sup>64</sup>Cu complexes were retained to a degree in the kidneys of mice, with a 40% retention of <sup>64</sup>Cu-NOTI after 40 minutes. This retention was greater than that of non-chelated <sup>64</sup>Cu indicating that it is the complex being retained and not due to the release of the metal. In contrast the retention of the complexes in the liver is slightly lower than that of free <sup>64</sup>Cu 45 minutes post injection, with only 11% of NOTI being retained whereas 17% of free copper was retained. This retention may be due to the overall positive charge of the complex in contrast to the negatively charged NOTA and DOTA complexes which are cleared from both organs.<sup>131</sup>

The successes seen when adapting CB-TE2A to CB-TE1A1P and CB-TE2P were not mirrored when Yoo and coworkers attempted to improve upon the radiolabelling conditions of the highly stable PCB-TE2A.<sup>119</sup> Whilst Cu-PCB-TE1A1P<sup>122</sup> and Cu-PCB-TE2P<sup>123</sup> both displayed a high stability under acidic conditions (Table 7), neither ligand significantly improved upon the high temperatures required for radiolabelling PCB-TE2A with <sup>64</sup>Cu(II).<sup>122,123</sup>

3.2.2. Non-macrocylic <sup>64</sup>Cu chelators. Orvig and coworkers applied H<sub>2</sub>dedpa to the complexation of <sup>64</sup>Cu.<sup>83</sup> As expected for an acyclic ligand, the radiolabelling conditions required were relatively mild – proceeding at room temperature and pH 5.5 – and a quantitative yield was rapidly achieved.<sup>83</sup> However the resulting complex had poor kinetic stability, degrading in 6 M HCl with a half-life less than 5 minutes.<sup>83</sup> Orvig and coworkers incorporated an alkyne into the H<sub>2</sub>dedpa ligand to facilitate bioconjugation through a catalysed azide–alkyne “Click” reaction.<sup>87</sup> To establish the stability of metal complexes formed with ligands conjugated in this way, benzyl azide was used to form the ligand H<sub>2</sub>azapa.<sup>87</sup> During the conjugation reaction it was noted that an excess of copper was needed due to complexation of Cu(II) ions by the ligand. After removal of the Cu(II) ions the H<sub>2</sub>azapa ligand was obtained and the stability of the copper complex that resulted was tested. Radiolabelling of H<sub>2</sub>azapa was successful, although significantly higher concentrations of ligand (182 mM) were needed<sup>87</sup> when compared to H<sub>2</sub>dedpa (10 μM).<sup>83</sup>

Comba and co-workers reported a range of bispidine chelates (Fig. 7) that could complex <sup>64</sup>Cu(II) extremely rapidly at room temperature (Table 8).<sup>140</sup> These

chelates also showed a high stability to transchelation by cyclam in a competition study<sup>140</sup> – L<sup>8</sup> retained 81% of the <sup>64</sup>Cu after 2 hours and 30% after 24 hours when incubated with 80 equivalents of cyclen, but L<sup>13</sup> retained 99% even after 24 hours incubation.<sup>140</sup> Overall the pentadentate chelates were shown to be more stable than their tetradentate counterparts to transchelation by cyclen.<sup>140</sup> In addition, the reduction of the bridging ketone to an alcohol improved the stability to transchelation – it was suggested that this prevented a reverse Mannich reaction which would cause the complex to decompose.<sup>140</sup> The stability of a number of these Cu-bispidine complexes were also tested against superoxide dismutase and in human serum.<sup>139</sup> 80% of the Cu-L<sup>10</sup> complex remained intact after an hour in human serum, however the p-OMe derivative L<sup>11</sup> formed a complex that showed a greater stability – with 96% remaining intact over an hour.<sup>139</sup> This trend was also seen in the transchelation studies previously mentioned.<sup>140</sup> These complexes also displayed very rapid radiolabelling kinetics – with labelling being completed in under a minute at room temperature for L<sup>8</sup>–L<sup>13</sup>.<sup>140</sup>

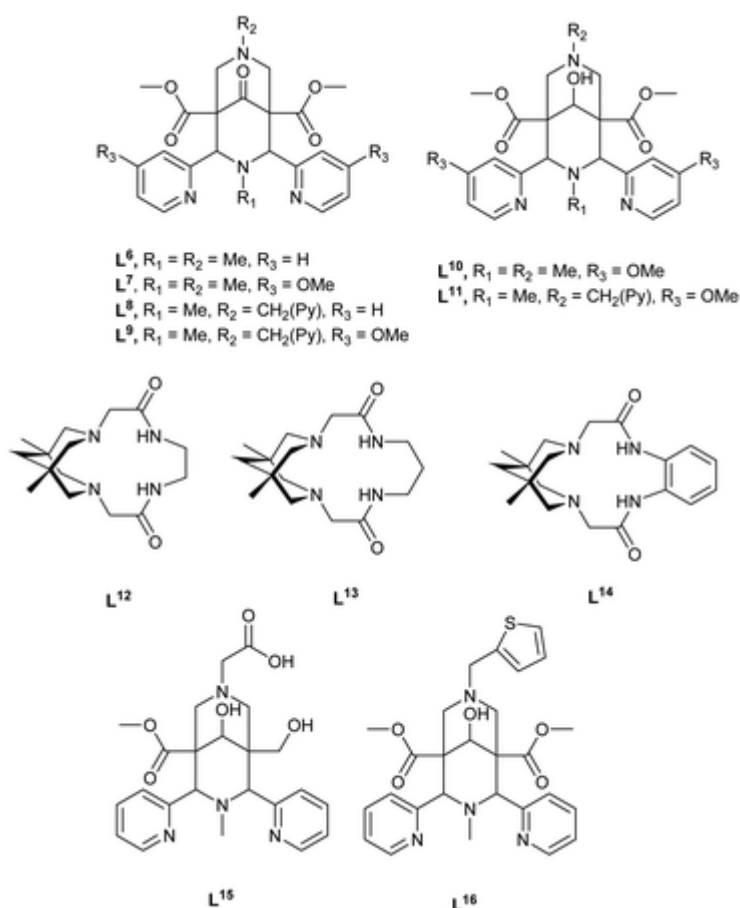


**Fig. 7** Bispidines applied to copper chelation.

Adaptation of bispidines to be incorporated into macrocycles significantly hampered the radiolabelling kinetics. L<sup>14</sup>, L<sup>15</sup> and L<sup>16</sup> (Fig. 7), all required heating to

50 °C to achieve a high radiochemical yield, with reaction times in excess of 30 minutes in each case.<sup>139</sup> However, L<sup>16</sup> was stable to superoxide dismutase and human serum, retaining 98.5 and 97.7% of the <sup>64</sup>Cu respectively after 1 hour in solution.<sup>139</sup>

Charbonnière and co-workers developed a pair of highly stable bispidine compounds – L<sup>15</sup> and L<sup>16</sup> (Fig. 7) – that showed extremely long copper-complex half-lives under acidic conditions.<sup>141</sup> These compounds have the same core as those described by Comba and co-workers,<sup>140</sup> with the pendant arms being varied to a carboxylic acid and a thiofuran. The 71 day half-life of Cu-L<sup>15</sup> under acidic conditions<sup>141</sup> demonstrates that it is kinetically inert, although radiolabelling has not yet been reported with this compound.

### 3.3. The future development of <sup>64</sup>Cu chelators

The development of chelators such as PCB-TE2A<sup>119</sup> for copper chelation which display a high kinetic stability is extremely promising for the future development of this field. Due to its long half-life, <sup>64</sup>Cu is well suited to longer studies involving targeting motifs with a longer biological half-life, such as antibodies. As a result, the copper-chelate complex formed needs to be highly stable in vivo. It is apparent that a cross-bridged cyclam motif is the most ideal form tested so far – and that adaptations of the cross bridge can produce highly stable complexes, such as PCB-TE2A and DPE-CB-DO2A. Further investigation into these chelates to further improve upon their radiolabelling conditions will be a key area of research for the development of copper chelates of the future.

Comba and coworkers reported bispidine ligands that rapidly complexed <sup>64</sup>Cu,<sup>140</sup> whereas Charbonnière and coworkers have reported highly stable Cu-bispidine complexes.<sup>141</sup> This class of chelator has not yet been widely explored for <sup>64</sup>Cu chelation but these early reports are highly promising.

The longer half-life of <sup>64</sup>Cu in comparison to <sup>68</sup>Ga and <sup>18</sup>F is more forgiving during the radiolabelling step; mild conditions that are tolerable by a wider range of targeting motifs is of a higher priority than extremely short complexation times. Significant progress has been made with respect to this goal – the development of CB-TE2P by Anderson et al. provides a clear example of how this goal may be achieved for other chelates in the future – careful selection of coordinating arms can lead to the optimisation of the complexation properties, for example improving the radiolabelling conditions without sacrificing stability of the resulting complex.

## 4. Zirconium-89

With a half-life of 3.3 days,  $^{89}\text{Zr}$  offers very different decay properties to  $^{68}\text{Ga}$  and  $^{64}\text{Cu}$ .<sup>9</sup> This longer half-life lends itself to techniques such as antibody based imaging where the biological lifetime is also several days.<sup>142</sup>  $^{89}\text{Zr}$  is produced using a cyclotron, this longer half-life also makes it more practical to transport the radioisotope from an external site if the scanning location does not have access to a cyclotron.<sup>143</sup>

Zr(IV) has complex aqueous chemistry, with a number of polynuclear species being formed<sup>144,145</sup> and poor solubility except at extreme pH values.<sup>146</sup> Weakly coordinated  $^{89}\text{Zr(IV)}$  has been shown to have an affinity for bones and joints,<sup>147</sup> and was also seen to accumulate in the liver under some conditions.<sup>147,148</sup> Zr(IV) will typically have a coordination number of 8.<sup>8,149</sup>

#### 4.1. Deferoxamine B

The majority of studies involving the chelation of  $^{89}\text{Zr}$  use the siderophore deferoxamine B (DFO – Fig. 8) as the chelator.<sup>148,150–158</sup>  $^{89}\text{Zr-DFO}$  showed good stability in vivo,<sup>159–162</sup> although recent studies have reported some bone uptake in mouse studies.<sup>148,150,153</sup> This instability is dependent on the method of conjugating DFO to the targeting motif – Tinianow and coworkers reported a 10.7% decomplexation over 6 days of  $^{89}\text{Zr}$  from a DFO complex where conjugation to trastuzumab was achieved through a CHX-maleimide linker,<sup>153</sup> whereas Zeglis and coworkers reported a 15.1% decomplexation over 5 days when a tetrazine/norbornene coupling reaction was used for conjugation to trastuzumab.<sup>150</sup>  $^{89}\text{Zr-DFO}$  has even been applied in man,<sup>163,164</sup> the successes of this ligand make it the prevailing choice for chelation of  $^{89}\text{Zr}$ .

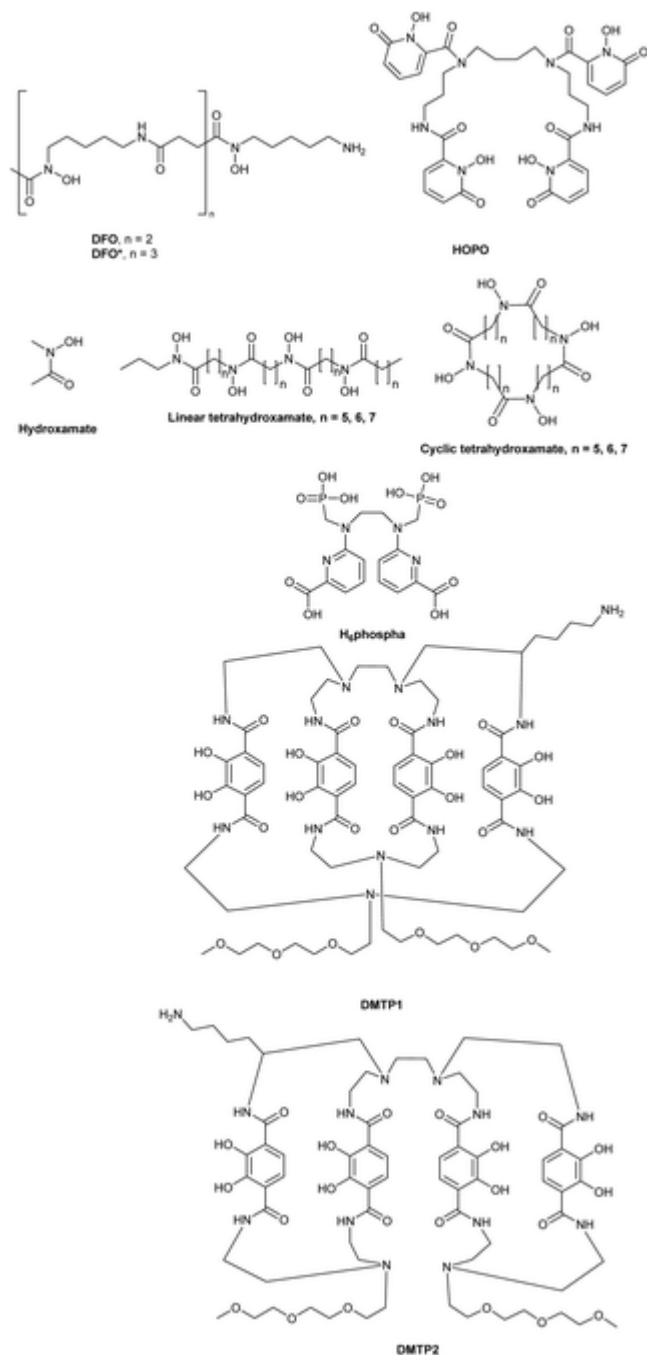


**Fig. 8** Structures of zirconium chelators.

Perk and coworkers achieved a 60% RCY when radiolabelling a DFO bioconjugate with <sup>89</sup>Zr in HEPES buffer.<sup>164</sup> In contrast, when using DTPA conjugated to the same antibody less than 0.1% labelling was observed.<sup>164</sup> Ma and coworkers achieved a 98% RCY when radiolabelling DFO in an ammonium acetate buffer (Table 9).<sup>159</sup>

**Table 9** Radiolabelling conditions and stability for <sup>89</sup>Zr chelates

Chelate	Radiolabelling conditions	RCY
DFO	RT, pH 7, 10 minutes, 1 mM	98 <sup>159</sup>
DFO*	RT, pH 7, 2 hours, 3 μM	100 <sup>165</sup>

Chelate	Radiolabelling conditions	RCY
HOPO	RT, pH 7, 10 minutes, 10 mM	100 <sup>162</sup>
Linear tetrahydroxamate n = 5	80 °C, pH 7, 30 minutes, 150 μM	87 <sup>161</sup>
Linear tetrahydroxamate n = 6	RT, pH 7, 2 hours, 150 μM	95 <sup>161</sup>
Linear tetrahydroxamate n = 7	RT, pH 7, 2 hours, 150 μM	99 <sup>161</sup>
Cyclic tetrahydroxamate n = 5	80 °C, pH 7, 30 minutes, 150 μM	29 <sup>161</sup>
Cyclic tetrahydroxamate n = 6	50 °C, pH 7, 30 minutes, 150 μM	92 <sup>161</sup>
Cyclic tetrahydroxamate n = 7	RT, pH 7, 2 hours, 150 μM	99 <sup>161</sup>
DMTP1	RT, pH 7, 15 minutes, 60 μM	100 <sup>160</sup>
DMTP2	RT, pH 7, 15 minutes, 60 μM	100 <sup>160</sup>
CP256	RT, pH 6.5, 10 minutes, 1 mM	99% <sup>159</sup>
FSC	RT, pH 7, 90 minutes, 58 μM	100 <sup>166</sup>
DTPA	RT, pH 7, 60 minutes	0.1 <sup>164</sup>
H <sub>6</sub> Phospha	37 °C, pH 7, 18 hours	12 <sup>167</sup>

---

#### 4.2. Alternative <sup>89</sup>Zr chelators

While Zr(IV) can accommodate up to 8 ligands in its coordination sphere, DFO occupies only 6 coordination sites. This has been speculated to be the cause of observed instability. An extended derivative of DFO, DFO\* (Fig. 8) has been synthesised and tested for its <sup>89</sup>Zr chelation ability.<sup>165</sup> A peptide conjugate of DFO\* was quantitatively radiolabelled at room temperature and pH 7 in 2 hours. The DFO\* complex remains largely intact after 24 hours in the presence of 3000 fold excess DFO (90% of the <sup>89</sup>Zr remaining complexed by DFO\*) showing that fully occupying the coordination sphere of zirconium can improve the stability of the resultant complex.<sup>165</sup>

10 mM HOPO (Fig. 8) was used to achieve quantitative radiolabelling with <sup>89</sup>Zr within 10 minutes at room temperature at pH 7.<sup>162</sup> However, as the concentration of the ligand was decreased, the complexation time increased. 10 μM of HOPO took 45 minutes to achieve quantitative complexation. The resultant <sup>89</sup>Zr-HOPO complex was extremely stable to transmetallation by EDTA, remaining completely intact when incubated with a 100 fold excess of EDTA across a range of pH values from 5–8 for over 7 days. The complex was also stable to transchelation by a range of metals, with iron being the notable exception with 17% of the <sup>89</sup>Zr being transchelated. No significant bone uptake (1%) of <sup>89</sup>Zr was seen over 24 hours in mice, and the complex underwent excretion via renal and hepatobiliary routes.

The crystal structure of zirconium with bidentate hydroxamates reveals that Zr(IV) forms an octacoordinated complex with 4 coordinated bidentate ligands.<sup>149</sup> As a result of this structure, a series of linear and cyclic tetrahydroxamic acid chelates were developed by Guérard and coworkers for the complexation of zirconium.<sup>161</sup> Unlike DFO, which has only 6 coordinating sites, these ligands would have 8 sites and therefore should form more stable complexes with Zr(IV). The length of the spacers between the coordination sites was varied to discern the optimum length – in this study it was found that a spacer length of 7 was more stable than one of 5.<sup>161</sup> The poor solubility of the complexes formed limited the characterisation that could be performed – however studies that made use of the radioactive <sup>89</sup>Zr isotope allowed for binding and stability studies to be performed. It was found that the largest cyclic tetrahydroxamic acid chelate could bind <sup>89</sup>Zr with a 92% RCY in 30 minutes at room temperature and pH 7, with a 99% yield after 2 hours. The smaller tetrahydroxamic acid ligands tested had reduced success at binding <sup>89</sup>Zr, although the linear analogues generally were more successful than the cyclic chelates. All chelates tested were stable to human serum and PBS over a 7 day period, but in the presence of concentrated EDTA the Zr(IV) was decomplexed to a degree for all systems tested. Both the cyclic and linear systems with a spacer length of 7 were more stable than DFO in the presence of EDTA (87%, 79% and 47% remaining after 7 days respectively). As expected, increasing the number of coordination sites improved the stability of the resulting zirconium complex.<sup>161</sup>

Blower et al. applied CP256 (Fig. 4) to the chelation of <sup>89</sup>Zr.<sup>159</sup> It was seen that CP256 formed a complex rapidly at room temperature and pH 6.5, with a 99% RCY at chelator concentrations above 1 mM. Below this concentration the labelling was significantly slower, at 100 µM it took 60 minutes to achieve a 9% RCY. Competition studies of CP256 with DFO showed that the complex formed was stable to transmetallation, with limited exchange to DFO when added to a <sup>89</sup>Zr-CP256 sample and rapid transmetallation when CP256 was added to a <sup>89</sup>Zr-DFO sample. In contrast, the CP256 complex was vulnerable to transchelation of the <sup>89</sup>Zr by Fe(III). When in a 10 : 1 [Fe] : [Zr-L] ratio, 86% of the Zr(IV) dissociated from the CP256 complex whereas only 7% dissociated from DFO. This is important as iron will be present in the body in much higher concentration than the complex when applied as a radiotracer. Testing of the CP256 complex in vivo showed that it rapidly cleared from the blood pool via a renal pathway. A bio-conjugated derivative of CP256, YM310-trastuzamab was labelled with <sup>89</sup>Zr and tested further. This system showed high stability in human serum, with >95% stability after 7 days. When tested in vivo in mice, however, the YM103-trastuzamab complex showed poorer stability, with 29.0% skeletal uptake being seen after 3 days.<sup>161</sup>

The success of the siderophore DFO inspired Decristoforo et al. to investigate the siderophore fusarine C (FSC).<sup>166</sup> The cyclic nature of this siderophore was expected to increase the stability of the resultant complex when compared to DFO. Radiolabelling in HEPES buffer at room temperature and neutral pH of FSC-RGD conjugates resulted in quantitative labelling with <sup>89</sup>Zr in 90 minutes at a concentration of 58 μM, and in 30 minutes at higher concentrations. The <sup>89</sup>Zr-FSC-RGD complexes showed high stability in PBS and human serum over a period of 7 days with no transmetallation being reported. In a solution containing 1000 fold excess EDTA, <sup>89</sup>Zr-FSC-RGD showed less than 6% transchelation over 7 days at pH 7. In contrast, <sup>89</sup>Zr-DFO showed nearly 60% transchelation by EDTA after 7 days. This indicates a much greater stability of FSC than DFO, highlighted in a competition study in which 100% transchelation of Zr-DFO occurred in the presence of 1000 fold FSC after 7 days, but only 40% when the ratios were reversed.<sup>166</sup>

A pair of large di-macrocyclic terephthalamide ligands were synthesised for zirconium chelation.<sup>160</sup> These chelates achieved quantitative labelling in 15 minutes at room temperature and neutral pH. In addition, the radiolabelling of these chelates was achieved at a much lower concentration of ligand than the radiolabelling of DFO. The resultant complex was highly stable in human serum over 7 days, and also stable to 50 mM DTPA at pH 7 for 7 days. <sup>89</sup>Zr-DFO was nearly 60% decomplexed under the same conditions.<sup>160</sup>

### 4.3. Future development of zirconium-89 chelators

Overall, chelation of <sup>89</sup>Zr has leapt forward over the last 5 years – going from just one recognised chelator to a range of alternative chelator systems. Further improvement of complexation times and complex stability can be expected, and further in vivo testing of those chelates that have been shown to be effective will cement their role for the future.

It is apparent that the use of cyclic chelators, and of occupying all 8 coordination sites of zirconium, are key to producing a highly stable complex. While both <sup>89</sup>Zr-DFO\* and <sup>89</sup>Zr-FSC showed improved stability when compared to <sup>89</sup>Zr-DFO, their extended radiolabelling times may limit their future use. However, the two dimacrocyclic terephthalamide ligands DMTP1 and DMTP2 have improved radiolabelling and stability properties when compared to DFO.<sup>160</sup> These ligands are highly promising and further studies into their in vivo behaviour will reveal whether or not they can truly compete with DFO as a chelator for <sup>89</sup>Zr.

## 5. Scandium-44

$^{44}\text{Sc}$  is a positron emitting isotope which has great potential. With a half-life of 3.9 hours,  $^{44}\text{Sc}$  can be used to study longer biological processes than  $^{68}\text{Ga}$ . In addition to this, another isotope of scandium,  $^{47}\text{Sc}$ , emits  $\beta^-$  and can be used as a therapeutic agent for treatment of cancers. The combination of these two isotopes would make a powerful medicinal tool as the distribution of the therapeutic agent could be followed exactly through the use of the PET agent.

$^{44}\text{Sc}$  can be produced from either a generator or a cyclotron source. Generator produced  $^{44}\text{Sc}$  is eluted from  $^{44}\text{Ti}$  (half-life = 59 years) using an ammonium acetate solution.<sup>168</sup> Cyclotron produced  $^{44}\text{Sc}$  is produced from a  $^{44}\text{Ca}$  target.<sup>169,170</sup> This variety of production methods makes scandium a versatile radiometal that could be widely used in the future, with the source being selected according to the user's requirements.

Scandium has a flexible coordination number, complexes with coordination 3 to 9 have been reported, although octahedral 6 coordinate complexes are the most common structure reported.<sup>171,172</sup> The chelation of scandium has not, until recently, been widely explored. Since 2012 a number of papers have been published exploring the chelation of  $^{44}\text{Sc}$  by common chelators.

### 5.1. $^{44}\text{Sc}$ chelators

DOTA and its derivatives have been applied to scandium and form stable complexes ( $\log K_{\text{Sc-DOTA}} = 27.0$ ) that remain stable to human serum over extended periods of time.<sup>173</sup> However, labelling requires heating and extended reaction times<sup>12</sup> – Majkowska-Pilip et al. reported labelling requiring temperatures of 70 °C and a labelling time of 30 minutes.<sup>173</sup> Labelling at room temperature was shown to be possible, although it required labelling times of over 24 hours.<sup>173</sup> NOTA was labelled significantly faster under these conditions, although the less stable complex formed resulted in a lower final yield of only 80%.<sup>173</sup> The  $^{44}\text{Sc}$ -NOTA complex formed was stable to human serum, although not to PBS due to the phosphate ions binding in place of the NOTA ligand.<sup>173</sup> Multiple studies have been carried out with  $^{44}\text{Sc}$ -DOTA type complexes in vivo, these show that the complex is highly stable and shows good specificity for its targets.<sup>12,174–177</sup>

Acyclic chelators have been shown to bind scandium more rapidly than DOTA,<sup>178,179</sup> although some chelators showed reduced stability when compared to cyclic chelators (Fig. 9).<sup>179</sup> CHX-A''-DTPA, DTPA and EGTA (Table 10) were all shown to be viable options for chelation of scandium. DTPA and EGTA achieved quantitative chelation at room temperature and the resulting complexes showed a high stability to PBS.<sup>179</sup> CHX-A''-DTPA (Table 10) achieved an 80% RCY in 30 minutes at pH 4.5 at room temperature.<sup>178</sup> When CHX-A''-DTPA was conjugated to a cetuximab-fab fragment the yield fell to 66%. DOTA-cetuximab-fab achieved only

a 21% RCY under these conditions, and NOTA-cetuximab-fab only a 14% yield.<sup>178</sup> The resulting <sup>44</sup>Sc-CHX-A''-DTPA complex showed high stability to mouse serum, with 92% of the complex remaining intact after 6 hours incubation.<sup>178</sup>

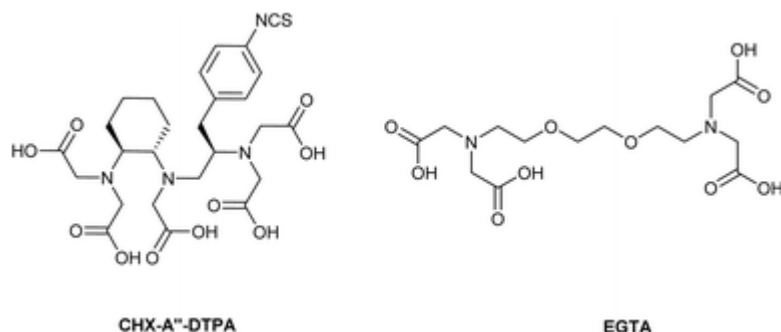


**Fig. 9** Acyclic scandium chelators.

**Table 10** Radiolabelling conditions for <sup>44</sup>Sc chelators

Chelator	Log K <sub>ML</sub>	Labelling conditions	RCY/%
DOTA	27.0 <sup>173</sup>	90 °C, pH 4.5, 15 minutes, 10 μM	97.7 <sup>12</sup>
NOTA	16.5 <sup>173</sup>	70 °C, pH 6, 30 minutes	80 <sup>173</sup>
CHX-A''-DTPA	—	RT, pH 4.5, 30 minutes, 1.6 μM	80 <sup>178</sup>
DTPA	—	RT, pH 6, 10 minutes	100 <sup>179</sup>
EGTA	—	RT, pH 6, 10 minutes	97.2 <sup>179</sup>

## 5.2. Future development of <sup>44</sup>Sc chelators

Overall, the limited development of <sup>44</sup>Sc chelators has shown that this radiometal has potential, with stable complexes formed under mild conditions. Macrocyclic chelators like DOTA have been shown to be able to bind <sup>44</sup>Sc, although these macrocyclic ligands require high temperatures for radiolabelling. CHX-A''-DTPA is an example of a chelator which will rapidly form complexes with scandium and appears to have a high stability. However, the stability of the <sup>44</sup>Sc-CHX-A''-DTPA complex has only been tested for 2 halflives – the complex will need to be stable for longer periods of time to be widely used in medical applications.

Development of the chelation of <sup>44</sup>Sc could be expanded through the application of many of the chelates discussed above. The chelates described here all contain a mixture of amine and acetic acid units – the use of alternate coordinating arms can change the radiolabelling kinetics and stability of the resulting complex significantly. The stability of <sup>44</sup>Sc-DOTA suggests that derivatives of this system would be a good starting point for future development.

Alternatively, stable acyclic chelate complexes could become the focus of development – the applicability of CP256 to both  $^{68}\text{Ga}$  and  $^{89}\text{Zr}$  complexation may translate to successful  $^{44}\text{Sc}$  complexation.

## 6. Conclusions

The trend towards shorter complexation times, under milder conditions has been apparent across the radiometals investigated and looks set to continue into the future, with effective labelling using lower ligand concentrations being an extension of this aim.

Due to its generator based production,  $^{68}\text{Ga}$  is set to become a widely used and readily accessible radionuclide for PET. The variety of acyclic chelators tested for their ability to complex  $^{68}\text{Ga}$  reflects the importance of rapid chelation for this radionuclide due to its relatively short half-life (68 minutes). Of the recently reported acyclic chelators CP256,<sup>45</sup> AAZTA<sup>91</sup> and H<sub>2</sub>dedpa<sup>4</sup> stand out for their mild and rapid radiolabelling conditions – and of these CP256 displays a particularly high stability to transchelation by transferrin which makes it promising for future development.

The longer half-life (12.7 hours), of  $^{64}\text{Cu}$  in comparison to  $^{68}\text{Ga}$  and  $^{18}\text{F}$  is more forgiving during the radiolabelling step; a highly stable  $^{64}\text{Cu}$  complex and mild conditions that are tolerable by a wider range of targeting motifs are of a higher priority than extremely rapid complexation kinetics. Significant progress has been made with respect to this goal – the development of CB-TE2P by Anderson et al.<sup>121</sup> provides a clear example of how this goal may be achieved for other chelates in the future. A measure of success has been with the bispidine species alongside modified cross-bridged species such as PCB-TE2A<sup>119</sup> and DPE-CB-TE2A<sup>132</sup> as the most successful chelates for  $^{64}\text{Cu}$ . Once a satisfactory stability is achieved, the next aim for  $^{64}\text{Cu}$  chelation would be to improve its complexation kinetics to improve the specific activity achieved and to reduce exposure of workers to unnecessary radiation. In this context PCB-TE2A<sup>119</sup> improves upon CB-TE2A but still requires harsh reaction conditions – however CB-TE2P<sup>121</sup> achieves almost quantitative complexation of  $^{64}\text{Cu}$  at room temperature in 30 minutes at ligand concentrations 3 orders of magnitude lower than that required for CB-TE2A.

Research into coordination of  $^{89}\text{Zr}$  has leapt forward over the last 5 years – going from just one recognised chelator to a range of alternative chelator systems. With its extremely long half-life rapid chelation kinetics do not need to be prioritised, kinetic and thermodynamic stability of the complex is key along with a specific targeting motif for imaging. Further improvement of complexation times and

complex stability can be expected, and further in vivo testing of those chelates that have been shown to be effective will cement their role for the future.

It is apparent that the use of cyclic chelators, and occupying all 8 coordination sites of zirconium, are key to producing a highly stable complex. While both  $^{89}\text{Zr}$ -DFO\* and  $^{89}\text{Zr}$ -FSC showed improved stability when compared to  $^{89}\text{Zr}$ -DFO, their extended radiolabelling times may limit their future use. However, the two dimacrocylic terephthalamide ligands DMTP1 and DMTP2 have improved radiolabelling and stability properties when compared to DFO.<sup>160</sup> These ligands are highly promising and further studies into their in vivo behaviour will reveal whether or not they can truly compete with DFO as a chelator for  $^{89}\text{Zr}$ . In addition to its success at complexation of  $^{68}\text{Ga}$ , CP256 has already been further applied to the complexation of another radiometal;  $^{89}\text{Zr}$ .<sup>159</sup> This ligand's versatility was demonstrated as it again formed a stable complex rapidly at room temperature – although the  $^{89}\text{Zr}$ -CP256 complex formed was vulnerable to transmetallation by  $\text{Fe}^{3+}$  ions.

$^{44}\text{Sc}$  is a positron emitting isotope which has great potential. With a half-life of 3.9 hours,  $^{44}\text{Sc}$  can be used to study longer biological processes than  $^{68}\text{Ga}$ . The success of traditional chelators at complexing scandium suggests that this will be a field that is ripe for development – much of the progress that has been seen for the other radiometals could be replicated using  $^{44}\text{Sc}$  to produce a PET tracer with a half-life that is between  $^{68}\text{Ga}$  and  $^{64}\text{Cu}$ , potentially increasing the flexibility of PET as a diagnostic technique.

Each of these radiometals have specific properties such as coordination geometry and half-life which should be considered when designing a new ligand system. This field is ever expanding and at an exciting juncture with significant advances in ligand design for Positron Emission Tomography Imaging.

## References

- 1 M. Partridge, A. Spinelli, W. Ryder and C. Hindorf, *Nucl. Instrum. Methods Phys. Res., Sect. A*, 2006, 568, 933–936.
- 2 G. F. Knoll, *Radiation detection and measurement: Glenn F. Knoll*, Wiley, Hoboken, N.J., 3rd edn, 2000.
- 3 P. W. Miller, N. J. Long, R. Vilar and A. D. Gee, *Angew. Chem., Int. Ed.*, 2008, 47, 8998–9033.
- 4 E. Boros, C. L. Ferreira, J. F. Cawthray, E. W. Price, B. O. Patrick, D. W. Wester, M. J. Adam and C. Orvig, *J. Am. Chem. Soc.*, 2010, 132, 15726–15733.
- 5 S. S. Gambhir, *Nat. Rev. Cancer*, 2002, 2, 683–693.
- 6 L. K. Shankar, J. M. Hoffman, S. Bacharach, M. M. Graham, J. Karp, A. A. Lammertsma, S. Larson, D. A. Mankoff, B. A. Siegel, A. Van den Abbeele, J. Yap and D. Sullivan, *J. Nucl. Med.*, 2006, 47, 1059–1066.
- 7 A. Bertoldo, G. Rizzo and M. Veronese, *Clin. Transl. Imaging*, 2014, 2, 239–251.
- 8 T. J. Wadas, E. H. Wong, G. R. Weisman and C. J. Anderson, *Chem. Rev.*, 2010, 110, 2858–2902.
- 9 G. Audi, O. Bersillon, J. Blachot and A. H. Wapstra, *Nucl. Phys. A*, 2003, 729, 3–128.
- 10 C. Champion and C. L. Loirec, *Phys. Med. Biol.*, 2007, 52, 6605.
- 11 A. K. Shukla and U. Kumar, *J. Med. Phys.*, 2006, 31, 13–21.
- 12 R. Hernandez, H. F. Valdovinos, Y. N. Yang, R. Chakravarty, H. Hong, T. E. Barnhart and W. B. Cai, *Mol. Pharm.*, 2014, 11, 2954–2961.
- 13 F. Roesch, *Curr. Radiopharm.*, 2012, 5, 187–201.
- 14 Y. Zhang, H. Hong and W. Cai, *Curr. Radiopharm.*, 2011, 4, 131–139.
- 15 L. R. Chervu and I. Sternlieb, *J. Nucl. Med.*, 1974, 15, 1011–1013.
- 16 W. R. Harris and V. L. Pecoraro, *Biochemistry*, 1983, 22, 292–299.
- 17 E. W. Price and C. Orvig, *Chem. Soc. Rev.*, 2014, 43, 260–290.
- 18 Z. Cai, B. T. Y. Li, E. H. Wong, G. R. Weisman and C. J. Anderson, *Dalton Trans.*, 2015, 44, 3945–3948.
- 19 M. D. Bartholoma, *Inorg. Chim. Acta*, 2012, 389, 36–51.
- 20 M. Fani, J. P. André and H. R. Maecke, *Contrast Media Mol. Imaging*, 2008, 3, 53–63.
- 21 P. J. Blower, J. S. Lewis and J. Zweit, *Nucl. Med. Biol.*, 1996, 23, 957–980.
- 22 C. F. Ramogida, C. L. Ferreira, J. F. Cawthray, C. Orvig and M. J. Adam, *Nucl. Med. Biol.*, 2014, 41, 632.
- 23 F. Zoller, P. J. Riss, F.-P. Montforts, D. K. Kelleher, E. Eppard and F. Rösch, *Nucl. Med. Biol.*, 2013, 40, 280–288.

- 24 H. L. Evans, Q.-D. Nguyen, L. S. Carroll, M. Kaliszczak, F. J. Twyman, A. C. Spivey and E. O. Aboagye, *Chem. Commun.*, 2014, 50, 9557–9560.
- 25 J. Kalia and R. T. Raines, *Curr. Org. Chem.*, 2010, 14, 138–147.
- 26 R. Vis, J. Lavalaye and E. van de Garde, *EJNMMI Res.*, 2015, 5, 27.
- 27 M. D. Bartholomä, A. S. Louie, J. F. Valliant and J. Zubieta, *Chem. Rev.*, 2010, 110, 2903–2920.
- 28 G. Bandoli, A. Dolmella, F. Tisato, M. Porchia and F. Refosco, *Coord. Chem. Rev.*, 2009, 253, 56–77.
- 29 Y. Li, A. E. Martell, R. D. Hancock, J. H. Reibenspies, C. J. Anderson and M. J. Welch, *Inorg. Chem.*, 1996, 35, 404–414.
- 30 J. Notni, J. Simecek, P. Hermann and H. J. Wester, *Chem. – Eur. J.*, 2011, 17, 14718–14722.
- 31 S. V. Govindan, R. B. Michel, G. L. Griffiths, D. M. Goldenberg and M. J. Mattes, *Nucl. Med. Biol.*, 2005, 32, 513–519.
- 32 E. Wong, P. Caravan, S. Liu, S. J. Rettig and C. Orvig, *Inorg. Chem.*, 1996, 35, 715–724.
- 33 Y. Z. Sun, C. J. Anderson, T. S. Pajeau, D. E. Reichert, R. D. Hancock, R. J. Motekaitis, A. E. Martell and M. J. Welch, *J. Med. Chem.*, 1996, 39, 458–470.
- 34 K. Plössl, R. Chandra, W. Qu, B. P. Lieberman, M.-P. Kung, R. Zhou, B. Huang and H. F. Kung, *Nucl. Med. Biol.*, 2008, 35, 83–90.
- 35 G. J. Stasiuk and N. J. Long, *Chem. Commun.*, 2013, 49, 2732–2746.
- 36 Z. Liu, Y. Yan, S. Liu, F. Wang and X. Chen, *Bioconjugate Chem.*, 2009, 20, 1016–1025.
- 37 R. Delgado, Y. Sun, R. J. Motekaitis and A. E. Martell, *Inorg. Chem.*, 1993, 32, 3320–3326.
- 38 R. Ma, M. J. Welch, J. Reibenspies and A. E. Martell, *Inorg. Chim. Acta*, 1995, 236, 75–82.
- 39 V. Kubíček, J. Havlíčková, J. Kotek, G. Tircsó, P. Hermann, É. Tóth and I. Lukeš, *Inorg. Chem.*, 2010, 49, 10960–10969.
- 40 E. T. Clarke and A. E. Martell, *Inorganica Chim. Acta*, 1991, 190, 37–46.
- 41 R. Delgado, M. D. Figueira and S. Quintino, *Talanta*, 1997, 45, 451–462.
- 42 R. Motekaitis, Y. Sun, A. E. Martell and M. J. Welch, *Inorg. Chem.*, 1991, 30, 2737–2740.
- 43 J. Simecek, M. Schulz, J. Notni, J. Plutnar, V. Kubicek, J. Havlickova and P. Hermann, *Inorg. Chem.*, 2012, 51, 577–590.
- 44 J. Simecek, J. Notni, T. G. Kapp, H. Kessler and H. J. Wester, *Mol. Pharm.*, 2014, 11, 1687–1695.
- 45 D. J. Berry, Y. M. Ma, J. R. Ballinger, R. Tavare, A. Koers, K. Sunassee, T. Zhou, S. Nawaz, G. E. D. Mullen, R. C. Hider and P. J. Blower, *Chem. Commun.*, 2011, 47, 7068–7070.
- 46 W. P. Jencks and J. Regenstein, in *Handbook of Biochemistry and Molecular Biology*, CRC Press, 4th edn, 2010, pp. 595–635, DOI: 10.1201/b10501-74.
- 47 M. Fellner, R. Baum, V. Kubíček, P. Hermann, I. Lukeš, V. Prasad and F. Rösch, *Eur. J. Nucl. Med. Mol. Imaging*, 2010, 37, 834–834.

- 48 M. Fani, A. Mueller, M. L. Tamma, G. Nicolas, H. R. Rink, R. Cescato, J. C. Reubi and H. R. Maecke, *J. Nucl. Med.*, 2010, 51, 1771–1779.
- 49 R. A. Dumont, F. Deininger, R. Haubner, H. R. Maecke, W. A. Weber and M. Fani, *J. Nucl. Med.*, 2011, 52, 1276–1284.
- 50 M. Fani, L. Del Pozzo, K. Abiraj, R. Mansi, M. L. Tamma, R. Cescato, B. Waser, W. A. Weber, J. C. Reubi and H. R. Maecke, *J. Nucl. Med.*, 2011, 52, 1110–1118.
- 51 I. Velikyan, A. Sundin, B. Eriksson, H. Lundqvist, J. Sorensen, M. Bergstrom and B. Langstrom, *Nucl. Med. Biol.*, 2010, 37, 265–275.
- 52 R. Srirajaskanthan, I. Kayani, A. M. Quigley, J. Soh, M. E. Caplin and J. Bomanji, *J. Nucl. Med.*, 2010, 51, 875–882.
- 53 V. Ambrosini, M. Zompatori, F. De Luca, D. Antonia, V. Allegri, C. Nanni, D. Malvi, E. Tonveronachi, L. Fasano, M. Fabbri and S. Fanti, *J. Nucl. Med.*, 2010, 51, 1950–1955.
- 54 V. Ambrosini, D. Campana, L. Bodei, C. Nanni, P. Castellucci, V. Allegri, G. C. Montini, P. Tomassetti, G. Paganelli and S. Fanti, *J. Nucl. Med.*, 2010, 51, 669–673.
- 55 D. Campana, V. Ambrosini, R. Pezzilli, S. Fanti, A. M. M. Labate, D. Santini, C. Ceccarelli, F. Nori, R. Franchi, R. Corinaldesi and P. Tomassetti, *J. Nucl. Med.*, 2010, 51, 353–359.
- 56 I. Velikyan, H. Maecke and B. Langstrom, *Bioconjugate Chem.*, 2008, 19, 569–573.
- 57 C. L. Ferreira, E. Lamsa, M. Woods, Y. Duan, P. Fernando, C. Bensimon, M. Kordos, K. Guenther, P. Jurek and G. E. Kiefer, *Bioconjugate Chem.*, 2010, 21, 531–536.
- 58 C. L. Ferreira, D. T. T. Yapp, D. Mandel, R. K. Gill, E. Boros, M. Q. Wong, P. Jurek and G. E. Kiefer, *Bioconjugate Chem.*, 2012, 23, 2239–2246.
- 59 K. Suzuki, M. Satake, J. Suwada, S. Oshikiri, H. Ashino, H. Dozono, A. Hino, H. Kasahara and T. Minamizawa, *Nucl. Med. Biol.*, 2011, 38, 1011–1018.
- 60 K. P. Eisenwiener, M. I. M. Prata, I. Buschmann, H. W. Zhang, A. C. Santos, S. Wenger, J. C. Reubi and H. R. Maecke, *Bioconjugate Chem.*, 2002, 13, 530–541.
- 61 K. Pohle, J. Notni, J. Bussemer, H. Kessler, M. Schwaiger and A. J. Beer, *Nucl. Med. Biol.*, 2012, 39, 777–784.
- 62 J. Notni, K. Pohle and H.-J. Wester, *EJNMMI Res.*, 2012, 2, 28.
- 63 J. Notni, P. Hermann, J. Havlickova, J. Kotek, V. Kubicek, J. Plutnar, N. Loktionova, P. J. Riss, F. Rosch and I. Lukes, *Chem. – Eur. J.*, 2010, 16, 7174–7185.
- 64 J. Notni, K. Pohle and H. J. Wester, *Nucl. Med. Biol.*, 2013, 40, 33–41.
- 65 Z. Baranyai, D. Reich, A. Vagner, M. Weineisen, I. Toth, H.-J. Wester and J. Notni, *Dalton Trans.*, 2015, 44, 11137–11146.
- 66 J. Notni, P. Hermann, I. Dregely and H. J. Wester, *Chem. – Eur. J.*, 2013, 19, 12602–12606.
- 67 J. Notni, J. Simecek and H. J. Wester, *ChemMedChem*, 2014, 9, 1107–1115.
- 68 J. Šimeček, O. Zemek, P. Hermann, J. Notni and H.-J. Wester, *Mol. Pharm.*, 2014, 11, 3893–3903.

- 69 M. T. Ma, O. C. Neels, D. Denoyer, P. Roselt, J. A. Karas, D. B. Scanlon, J. M. White, R. J. Hicks and P. S. Donnelly, *Bioconjugate Chem.*, 2011, 22, 2093–2103.
- 70 L. Wei, Y. Miao, F. Gallazzi, T. P. Quinn, M. J. Welch, A. L. Vāvere and J. S. Lewis, *Nucl. Med. Biol.*, 2007, 34, 945–953.
- 71 W. Breeman, M. Jong, E. Blois, B. Bernard, M. Konijnenberg and E. Krenning, *Eur. J. Nucl. Med. Mol. Imaging*, 2005, 32, 478–485.
- 72 S. Poty, P. Désogère, J. Šimeček, C. Bernhard, V. Goncalves, C. Goze, F. Boschetti, J. Notni, H. J. Wester and F. Denat, *ChemMedChem*, 2015, 10, 1475–1479.
- 73 B. Behnam Azad, C.-F. Cho, J. D. Lewis and L. G. Luyt, *Appl. Radiat. Isot.*, 2012, 70, 505–511.
- 74 M. Bhadwal, T. Das, H. Dev Sarma and S. Banerjee, *Mol. Imaging Biol.*, 2015, 17, 111–118.
- 75 F. Bryden, H. Savoie, E. V. Rosca and R. W. Boyle, *Dalton Trans.*, 2015, 44, 4925–4932.
- 76 Y. Fazaeli, A. R. Jalilian, M. M. Amini, K. Ardaneh, A. Rahiminejad, F. Bolourinovin, S. Moradkhani and A. Majdabadi, *Nucl. Med. Mol. Imaging*, 2012, 46, 20–26.
- 77 J. Holub, M. Meckel, V. Kubíček, F. Rösch and P. Hermann, *Contrast Media Mol. Imaging*, 2015, 10, 122–134.
- 78 M. Petrik, H. Haas, G. Dobrozemsky, C. Lass-Flörl, A. Helbok, M. Blatzer, H. Dietrich and C. Decristoforo, *J. Nucl. Med.*, 2010, 51, 639–645.
- 79 M. Petrik, H. Haas, M. Schrettl, A. Helbok, M. Blatzer and C. Decristoforo, *Nucl. Med. Biol.*, 2012, 39, 361–369.
- 80 M. Petrik, G. Franssen, H. Haas, P. Laverman, C. Hörtnagl, M. Schrettl, A. Helbok, C. Lass-Flörl and C. Decristoforo, *Eur. J. Nucl. Med. Mol. Imaging*, 2012, 39, 1175–1183.
- 81 C. Zhai, D. Summer, C. Rangger, H. Haas, R. Haubner and C. Decristoforo, *J. Labelled Compd. Radiopharm.*, 2015, 58, 209–214.
- 82 P. A. Knetsch, C. Zhai, C. Rangger, M. Blatzer, H. Haas, P. Kaeopookum, R. Haubner and C. Decristoforo, *Nucl. Med. Biol.*, 2015, 42, 115–122.
- 83 E. Boros, J. F. Cawthray, C. L. Ferreira, B. O. Patrick, M. J. Adam and C. Orvig, *Inorg. Chem.*, 2012, 51, 6279–6284.
- 84 E. Boros, C. L. Ferreira, B. O. Patrick, M. J. Adam and C. Orvig, *Nucl. Med. Biol.*, 2011, 38, 1165–1174.
- 85 E. Boros, C. L. Ferreira, D. T. T. Yapp, R. K. Gill, E. W. Price, M. J. Adam and C. Orvig, *Nucl. Med. Biol.*, 2012, 39, 785–794.
- 86 C. F. Ramogida, J. F. Cawthray, E. Boros, C. L. Ferreira, B. O. Patrick, M. J. Adam and C. Orvig, *Inorg. Chem.*, 2015, 54, 2017–2031.
- 87 G. A. Bailey, E. W. Price, B. M. Zeglis, C. L. Ferreira, E. Boros, M. J. Lacasse, B. O. Patrick, J. S. Lewis, M. J. Adam and C. Orvig, *Inorg. Chem.*, 2012, 51, 12575–12589.
- 88 L. Tei, G. Gugliotta, M. Fekete, F. K. Kalman and M. Botta, *Dalton Trans.*, 2011, 40, 2025–2032.

- 89 Z. Baranyai, F. Uggeri, A. Maiocchi, G. B. Giovenzana, C. Cavallotti, A. Takacs, I. Toth, I. Banyai, A. Benyei, E. Brucher and S. Aime, *Eur. J. Inorg. Chem.*, 2013, 147–162, DOI: 10.1002/ejic.201201108.
- 90 D. Parker, B. P. Waldron and D. S. Yufit, *Dalton Trans.*, 2013, 42, 8001–8008.
- 91 B. P. Waldron, D. Parker, C. Burchardt, D. S. Yufit, M. Zimny and F. Roesch, *Chem. Commun.*, 2013, 49, 579–581.
- 92 N. Vologdin, G. A. Rolla, M. Botta and L. Tei, *Org. Biomol. Chem.*, 2013, 11, 1683–1690.
- 93 D. Parker and B. P. Waldron, *Org. Biomol. Chem.*, 2013, 11, 2827–2838.
- 94 J. Seemann, B. P. Waldron, F. Roesch and D. Parker, *ChemMedChem*, 2015, 10, 1019–1026.
- 95 F. Silva, M. P. C. Campello, L. Gano, C. Fernandes, I. C. Santos, I. Santos, J. R. Ascenso, M. Joao Ferreira and A. Paulo, *Dalton Trans.*, 2015, 44, 3342–3355.
- 96 M. T. Ma, C. Cullinane, C. Imberti, J. Bagaña Torres, S. Y. A. Terry, P. Roselt, R. J. Hicks and P. J. Blower, *Bioconjugate Chem.*, 2015, DOI: 10.1021/acs.bioconjchem.5b00335.
- 97 R. L. Arrowsmith, P. A. Waghorn, M. W. Jones, A. Bauman, S. K. Brayshaw, Z. Hu, G. Kociok-Kohn, T. L. Mindt, R. M. Tyrrell, S. W. Botchway, J. R. Dilworth and S. I. Pascu, *Dalton Trans.*, 2011, 40, 6238–6252.
- 98 O. Thews, M. Zimny, E. Eppard, M. Piel, N. Bausbacher, V. Nagel and F. Rösch, *Mol. Imaging Biol.*, 2014, 16, 802–812.
- 99 M. Fellner, W. Dillenburger, H.-G. Buchholz, N. Bausbacher, M. Schreckenberger, F. Renz, F. Rösch and O. Thews, *Mol. Imaging Biol.*, 2011, 13, 985–994.
- 100 C. F. Ramogida, C. L. Ferreira, J. Cawthray, C. Orvig and M. J. Adam, *J. Labelled Comp. Radiopharm.*, 2013, 56, S197–S197.
- 101 C. J. Anderson and R. Ferdani, *Cancer Biother. Radiopharm.*, 2009, 24, 379–393.
- 102 D. W. McCarthy, R. E. Shefer, R. E. Klinkowstein, L. A. Bass, W. H. Margeneau, C. S. Cutler, C. J. Anderson and M. J. Welch, *Nucl. Med. Biol.*, 1997, 24, 35–43.
- 103 J. L. J. Dearling and P. J. Blower, *Chem. Commun.*, 1998, 2531–2532, DOI: 10.1039/A805957H.
- 104 H. Tapiero, D. M. Townsend and K. D. Tew, *Biomed. Pharmacother.*, 2003, 57, 386–398.
- 105 C. J. Mathias, M. J. Welch, M. A. Green, H. Diril, C. F. Meares, R. J. Gropler and S. R. Bergmann, *J. Nucl. Med.*, 1991, 32, 475–480.
- 106 D. K. Cabbiness and D. W. Margerum, *J. Am. Chem. Soc.*, 1969, 91, 6540–6541.
- 107 A. Bevilacqua, R. I. Gelb, W. B. Hebard and L. J. Zompa, *Inorg. Chem.*, 1987, 26, 2699–2706.
- 108 X. K. Sun, M. Wuest, Z. Kovacs, A. D. Sherry, R. Motekaitis, Z. Wang, A. E. Martell, M. J. Welch and C. J. Anderson, *J. Biol. Inorg. Chem.*, 2003, 8, 217–225.
- 109 J. Kotek, P. Lubal, P. Hermann, I. Cisarova, I. Lukes, T. Godula, I. Svobodova, P. Taborsky and J. Havel, *Chem. – Eur. J.*, 2003, 9, 233–248.

- 110 K. S. Woodin, K. J. Heroux, C. A. Boswell, E. H. Wong, G. R. Weisman, W. J. Niu, S. A. Tomellini, C. J. Anderson, L. N. Zakharov and A. L. Rheingold, *Eur. J. Inorg. Chem.*, 2005, 4829–4833, DOI: 10.1002/ejic.200500579.
- 111 D. C. Weatherburn, E. J. Billo, J. P. Jones and D. W. Margerum, *Inorg. Chem.*, 1970, 9, 1557–1559.
- 112 R. Ševčík, J. Vaněk, P. Lubal, Z. Kotková, J. Kotek and P. Hermann, *Polyhedron*, 2014, 67, 449–455.
- 113 K. Kumar, M. F. Tweedle, M. F. Malley and J. Z. Gougoutas, *Inorg. Chem.*, 1995, 34, 6472–6480.
- 114 X. K. Sun, M. Wuest, G. R. Weisman, E. H. Wong, D. P. Reed, C. A. Boswell, R. Motekaitis, A. E. Martell, M. J. Welch and C. J. Anderson, *J. Med. Chem.*, 2002, 45, 469–477.
- 115 S. A. Pisareva, F. I. Belskii, T. Y. Medved and M. I. Kabachnik, *Bull. Acad. Sci. USSR, Div. Chem. Sci.*, 1987, 36, 372–376.
- 116 T. J. Wadas and C. J. Anderson, *Nat. Protoc.*, 2007, 1, 3062–3068.
- 117 E. Boros, E. Rybak-Akimova, J. P. Holland, T. Rietz, N. Rotile, F. Blasi, H. Day, R. Latifi and P. Caravan, *Mol. Pharm.*, 2014, 11, 617–629.
- 118 J. Simecek, P. Hermann, J. Havlickova, E. Herdtweck, T. G. Kapp, N. Engelbogen, H. Kessler, H. J. Wester and J. Notni, *Chem. – Eur. J.*, 2013, 19, 7748–7757.
- 119 D. N. Pandya, A. V. Dale, J. Y. Kim, H. Lee, Y. S. Ha, G. I. An and J. Yoo, *Bioconjugate Chem.*, 2012, 23, 330–335.
- 120 J. Simecek, H. J. Wester and J. Notni, *Dalton Trans.*, 2012, 41, 13803–13806.
- 121 R. Ferdani, D. J. Stigers, A. L. Fiamengo, L. H. Wei, B. T. Y. Li, J. A. Golen, A. L. Rheingold, G. R. Weisman, E. H. Wong and C. J. Anderson, *Dalton Trans.*, 2012, 41, 1938–1950.
- 122 A. V. Dale, G. I. An, D. N. Pandya, Y. S. Ha, N. Bhatt, N. Soni, H. Lee, H. Ahn, S. Sarkar, W. Lee, P. T. Huynh, J. Y. Kim, M.-R. Gwon, S. H. Kim, J. G. Park, Y.-R. Yoon and J. Yoo, *Inorg. Chem.*, 2015, 54, 8177–8186.
- 123 N. Bhatt, N. Soni, Y. S. Ha, W. Lee, D. N. Pandya, S. Sarkar, J. Y. Kim, H. Lee, S. H. Kim, G. I. An and J. Yoo, *ACS Med. Chem. Lett.*, 2015, 6, 1162–1166.
- 124 A. Y. Odendaal, A. L. Fiamengo, R. Ferdani, T. J. Wadas, D. C. Hill, Y. Peng, K. J. Heroux, J. A. Golen, A. L. Rheingold, C. J. Anderson, G. R. Weisman and E. H. Wong, *Inorg. Chem.*, 2011, 50, 3078–3086.
- 125 L. M. P. Lima, D. Esteban-Gómez, R. Delgado, C. Platas-Iglesias and R. Tripier, *Inorg. Chem.*, 2012, 51, 6916–6927.
- 126 M. Frindel, N. Camus, A. Rauscher, M. Bourgeois, C. Alliot, L. Barré, J.-F. Gestin, R. Tripier and A. Faivre-Chauvet, *Nucl. Med. Biol.*, 2014, 41(Supplement), e49–e57.
- 127 N. Wu, C. S. Kang, I. Sin, S. Ren, D. Lie, V. C. Ruthengael, M. R. Lewis and H.-S. Chong, *J. Biol. Inorg. Chem.*, 2015, DOI: 0.1007/s00775-015-1318-7, -8.
- 128 R. Bergmann, A. Ruffani, B. Graham, L. Spiccia, J. Steinbach, J. Pietzsch and H. Stephan, *Eur. J. Med. Chem.*, 2013, 70, 434–446.
- 129 M. Roger, L. M. P. Lima, M. Frindel, C. Platas-Iglesias, J. F. Gestin, R. Delgado, V. Patinec and R. Tripier, *Inorg. Chem.*, 2013, 52, 5246–5259.

- 130 K. Viehweger, L. Barbaro, K. P. García, T. Joshi, G. Geipel, J. Steinbach, H. Stephan, L. Spiccia and B. Graham, *Bioconjugate Chem.*, 2014, 25, 1011–1022.
- 131 C. Gotzmann, F. Braun and M. D. Bartholoma, *RSC Adv.*, 2016, 6, 119–131.
- 132 C. V. Esteves, P. Lamosa, R. Delgado, J. Costa, P. Desogere, Y. Rousselin, C. Goze and F. Denat, *Inorg. Chem.*, 2013, 52, 5138–5153.
- 133 L. M. P. Lima, Z. Halime, R. Marion, N. Camus, R. Delgado, C. Platas-Iglesias and R. Tripier, *Inorg. Chem.*, 2014, 53, 5269–5279.
- 134 D. J. Stigers, R. Ferdani, G. R. Weisman, E. H. Wong, C. J. Anderson, J. A. Golen, C. Moore and A. L. Rheingold, *Dalton Trans.*, 2010, 39, 1699–1701.
- 135 D. Zeng, Y. Guo, A. G. White, Z. Cai, J. Modi, R. Ferdani and C. J. Anderson, *Mol. Pharm.*, 2014, 11, 3980–3987.
- 136 D. Zeng, Q. Ouyang, Z. Cai, X.-Q. Xie and C. J. Anderson, *Chem. Commun.*, 2014, 50, 43–45.
- 137 K. Born, P. Comba, R. Ferrari, G. A. Lawrance and H. Wadepohl, *Inorg. Chem.*, 2007, 46, 458–464.
- 138 P. Comba, S. Hunoldt, M. Morgen, J. Pietzsch, H. Stephan and H. Wadepohl, *Inorg. Chem.*, 2013, 52, 8131–8143.
- 139 P. Comba, M. Kubeil, J. Pietzsch, H. Rudolf, H. Stephan and K. Zarschler, *Inorg. Chem.*, 2014, 53, 6698–6707.
- 140 P. Comba, F. Emmerling, M. Jakob, W. Kraus, M. Kubeil, M. Morgen, J. Pietzsch and H. Stephan, *Dalton Trans.*, 2013, 42, 6142–6148.
- 141 A. Roux, A. M. Nonat, J. Brandel, V. Hubscher-Bruder and L. J. Charbonnière, *Inorg. Chem.*, 2015, 54, 4431–4444.
- 142 C. A. Boswell and M. W. Brechbiel, *Nucl. Med. Biol.*, 2007, 34, 757–778.
- 143 A. Hohn, K. Zimmermann, E. Schaub, W. Hirzel, P. A. Schubiger and R. Schibli, *Q. J. Nucl. Med. Mol. Imaging*, 2008, 52, 145–150.
- 144 A. Singhal, L. M. Toth, J. S. Lin and K. Affholter, *J. Am. Chem. Soc.*, 1996, 118, 11529–11534.
- 145 T. Sasaki, T. Kobayashi, I. Takagi and H. Moriyama, *J. Nucl. Sci. Technol.*, 2008, 45, 735–739.
- 146 C. Ekberg, G. Källvenius, Y. Albinsson and P. Brown, *J. Solution Chem.*, 2004, 33, 47–79.
- 147 D. S. Abou, T. Ku and P. M. Smith-Jones, *Nucl. Med. Biol.*, 2011, 38, 675–681.
- 148 J. P. Holland, V. Divilov, N. H. Bander, P. M. Smith-Jones, S. M. Larson and J. S. Lewis, *J. Nucl. Med.*, 2010, 51, 1293–1300.
- 149 F. Guerard, Y.-S. Lee, R. Tripier, L. P. Szajek, J. R. Deschamps and M. W. Brechbiel, *Chem. Commun.*, 2013, 49, 1002–1004.
- 150 B. M. Zeglis, P. Mohindra, G. I. Weissmann, V. Divilov, S. A. Hilderbrand, R. Weissleder and J. S. Lewis, *Bioconjugate Chem.*, 2011, 22, 2048–2059.
- 151 L. R. Perk, M. Vosjan, G. W. M. Visser, M. Budde, P. Jurek, G. E. Kiefer and G. van Dongen, *Eur. J. Nucl. Med. Mol. Imaging*, 2010, 37, 250–259.

- 152 I. Verel, G. W. M. Visser, R. Boellaard, M. Stigter-van Walsum, G. B. Snow and G. A. M. S. van Dongen, *J. Nucl. Med.*, 2003, 44, 1271–1281.
- 153 J. N. Tinianow, H. S. Gill, A. Ogasawara, J. E. Flores, A. N. Vanderbilt, E. Luis, R. Vandlen, M. Darwish, J. R. Junutula, S.-P. Williams and J. Marik, *Nucl. Med. Biol.*, 2010, 37, 289–297.
- 154 J. P. Holland, M. J. Evans, S. L. Rice, J. Wongvipat, C. L. Sawyers and J. S. Lewis, *Nat. Med.*, 2012, 18, 1586–U1197.
- 155 T. H. Oude Munnink, M. E. A. Arjaans, H. TimmerBosscha, C. P. Schröder, J. W. Hesselink, S. R. Vedelaar, A. M. E. Walenkamp, M. Reiss, R. C. Gregory, M. N. Lub-de Hooge and E. G. E. de Vries, *J. Nucl. Med.*, 2011, 52, 2001–2008.
- 156 A. Ruggiero, J. P. Holland, T. Hudolin, L. Shenker, A. Koulova, N. H. Bander, J. S. Lewis and J. Grimm, *J. Nucl. Med.*, 2011, 52, 1608–1615.
- 157 B. A. W. Hoeben, J. H. A. M. Kaanders, G. M. Franssen, E. G. C. Troost, P. F. J. W. Rijken, E. Oosterwijk, G. A. M. S. v. Dongen, W. J. G. Oyen, O. C. Boerman and J. Bussink, *J. Nucl. Med.*, 2010, 51, 1076–1083.
- 158 A. Natarajan, F. Habte and S. S. Gambhir, *Bioconjugate Chem.*, 2012, 23, 1221–1229.
- 159 M. T. Ma, L. K. Meszaros, B. M. Paterson, D. J. Berry, M. S. Cooper, Y. Ma, R. C. Hider and P. J. Blower, *Dalton Trans.*, 2015, 44, 4884–4900.
- 160 D. N. Pandya, S. Pailloux, D. Tatum, D. Magda and T. J. Wadas, *Chem. Commun.*, 2015, 51, 2301–2303.
- 161 F. Guérard, Y.-S. Lee and M. W. Brechbiel, *Chem. – Eur. J.*, 2014, 20, 5584–5591.
- 162 M. A. Deri, S. Ponnala, B. M. Zeglis, G. Pohl, J. J. Dannenberg, J. S. Lewis and L. C. Francesconi, *J. Med. Chem.*, 2014, 57, 4849–4860.
- 163 E. C. Dijkers, T. H. Oude Munnink, J. G. Kosterink, A. H. Brouwers, P. L. Jager, J. R. de Jong, G. A. van Dongen, C. P. Schröder, M. N. Lub-de Hooge and E. G. de Vries, *Clin. Pharmacol. Ther.*, 2010, 87, 586–592.
- 164 L. Perk, O. Visser, M. Stigter-van Walsum, M. W. D. Vosjan, G. M. Visser, J. Zijlstra, P. Huijgens and G. M. S. van Dongen, *Eur. J. Nucl. Med. Mol. Imaging*, 2006, 33, 1337–1345.
- 165 M. Patra, A. Bauman, C. Mari, C. A. Fischer, O. Blacque, D. Haussinger, G. Gasser and T. L. Mindt, *Chem. Commun.*, 2014, 50, 11523–11525.
- 166 C. Zhai, D. Summer, C. Rangger, G. M. Franssen, P. Laverman, H. Haas, M. Petrik, R. Haubner and C. Decristoforo, *Mol. Pharm.*, 2015, 12, 2142–2150.
- 167 E. W. Price, B. M. Zeglis, J. S. Lewis, M. J. Adam and C. Orvig, *Dalton Trans.*, 2014, 43, 119–131.
- 168 M. Pruszyński, N. S. Loktionova, D. V. Filosofov and F. Rösch, *Appl. Radiat. Isot.*, 2010, 68, 1636–1641.
- 169 C. Alliot, R. Kerdjoudj, N. Michel, F. Haddad and S. Huclier-Markai, *Nucl. Med. Biol.*, 2015, 42, 524–529.
- 170 N. P. van der Meulen, M. Bunka, K. A. Domnanich, C. Müller, S. Haller, C. Vermeulen, A. Türler and R. Schibli, *Nucl. Med. Biol.*, 2015, 42, 745–751.

- 171 S. Cotton, *Polyhedron*, 1999, 18, 1691–1715.
- 172 P. R. Meehan, D. R. Aris and G. R. Willey, *Coord. Chem. Rev.*, 1999, 181, 121–145.
- 173 A. Majkowska-Pilip and A. Bilewicz, *J. Inorg. Biochem.*, 2011, 105, 313–320.
- 174 E. Koumariou, N. S. Loktionova, M. Fellner, F. Roesch, O. Thews, D. Pawlak, S. C. Archimandritis and Dalton Transactions R. Mikolajczak, *Appl. Radiat. Isot.*, 2012, 70, 2669–2676.
- 175 M. Pruszyński, A. Majkowska-Pilip, N. S. Loktionova, E. Eppard and F. Roesch, *Appl. Radiat. Isot.*, 2012, 70, 974–979.
- 176 C. Müller, M. Bunka, J. Reber, C. Fischer, K. Zhernosekov, A. Türler and R. Schibli, *J. Nucl. Med.*, 2013, 54, 2168–2174.
- 177 C. Muller, M. Bunka, S. Haller, U. Koster, V. Groehn, P. Bernhardt, N. van der Meulen, A. Turler and R. Schibli, *J. Nucl. Med.*, 2014, 55, 1658–1664.
- 178 R. Chakravarty, S. Goel, H. F. Valdovinos, R. Hernandez, H. Hong, R. J. Nickles and W. B. Cai, *Bioconjugate Chem.*, 2014, 25, 2197–2204.
- 179 M. Połosak, A. Piotrowska, S. Krajewski and A. Bilewicz, *J. Radioanal. Nucl. Chem.*, 2013, 295, 1867–1872